

2013

# The Influence of the Tibetan Plateau Elevation on the Global and Asian Monsoons

Rene Paul Acosta  
*Purdue University*

Follow this and additional works at: [https://docs.lib.purdue.edu/open\\_access\\_theses](https://docs.lib.purdue.edu/open_access_theses)



Part of the [Climate Commons](#), [Environmental Indicators and Impact Assessment Commons](#), [Geology Commons](#), and the [Meteorology Commons](#)

---

## Recommended Citation

Acosta, Rene Paul, "The Influence of the Tibetan Plateau Elevation on the Global and Asian Monsoons" (2013). *Open Access Theses*. 16.  
[https://docs.lib.purdue.edu/open\\_access\\_theses/16](https://docs.lib.purdue.edu/open_access_theses/16)

This document has been made available through Purdue e-Pubs, a service of the Purdue University Libraries. Please contact [epubs@purdue.edu](mailto:epubs@purdue.edu) for additional information.

**PURDUE UNIVERSITY**  
**GRADUATE SCHOOL**  
**Thesis/Dissertation Acceptance**

This is to certify that the thesis/dissertation prepared

By Rene Paul Acosta

Entitled

The Influence of the Tibetan Plateau on the global and Asian monsoons

For the degree of Master of Science

Is approved by the final examining committee:

Ernest Agee

Chair

Matthew Huber

Alex Gluhovsky

To the best of my knowledge and as understood by the student in the *Research Integrity and Copyright Disclaimer (Graduate School Form 20)*, this thesis/dissertation adheres to the provisions of Purdue University's "Policy on Integrity in Research" and the use of copyrighted material.

Approved by Major Professor(s): Ernest Agee

Approved by: Indrajeet Chaubey

Head of the Graduate Program

11/25/2013

Date



THE INFLUENCE OF THE TIBETAN PLATEAU ELEVATION ON THE GLOBAL AND ASIAN  
MONSOONS

A Thesis

Submitted to the Faculty

of

Purdue University

by

R. Paul Acosta

In Partial Fulfillment of the

Requirements for the Degree

of

Master of Science

December 2013

Purdue University

West Lafayette, Indiana

## ACKNOWLEDGEMENTS

I would like to thank Matthew Huber, Ernest Agee, and Alex Gluhovsky for their scientific mentorship. Also I thank Aaron Goldner, Jon Buzan, Peter Roberson, Ian Pope and Rachel Gipe for technical support. William Boos for his Himalayan Mountain configuration. Robin Blomdin for putting together figure 1a. Katie Bailey and Nicholas Herold for critically reading the manuscript.

## TABLE OF CONTENTS

	Page
LIST OF TABLES.....	v
LIST OF FIGURES.....	vi
ABSTRACT .....	ix
1. INTRODUCTION.....	1
2. BACKGROUND.....	7
2.1 Mountains and their influence on climate.....	7
2.2 Overview of Monsoon Systems.....	9
2.3 Literature Review on Tibetan Plateau simulations .....	14
3. METHODOLOGY .....	21
3.1 Experiment Design .....	23
3.2 Monsoon Indices.....	24
3.3 Observed Precipitation .....	25
4. RESULTS .....	27
4.1 Precipitation Biases.....	27
4.2 Influence of the Tibetan Plateau.....	29
4.2.1 Heating Over Asia .....	29

4.2.2 Divergence and Precipitation Over Asia .....	34
4.2.3 Mean and Transient Integrated Moisture Transport.....	41
4.3 Global Precipitation Distributions and the Global Monsoon Index .....	45
4.4 Preliminary CAM 5 comparisons .....	52
5. DISCUSSION .....	55
5.1 Precipitation regimes over Southern Asia.....	55
5.2 The Global Monsoon.....	58
5.3 CAM5 Comparison .....	61
6. CONCLUSION, FUTURE DIRECTIONS AND IMPLICATIONS.....	63
LIST OF REFERENCES .....	67

## LIST OF TABLES

Table	Page
Table 1: List of simulations and technical information .....	26
Table 2: Diagnostics variables taken from all modern simulations.....	61

## LIST OF FIGURES

Figure	Page
Figure 1: Displays the full extent of Tibetan Plateau, on a Lambert Conformal Conic projection with dark color as higher elevation (a). This image was from USGS GTOPO 30, assembled using ARC GIS by Robin Bloomdin. Image b, illustrates all five of our topographic configurations: Control, No-Plateau, Half-Plateau, Double-Plateau and Himalayan-Wall.....	2
Figure 2: Global precipitation distribution of Modern CESM CAM4 and GPCP 1979-2009 are shown in plots (a and b). Where as plots c and d shows the comparisons between the two. Plot (c) is a meridional transect with mean zonal global precipitations. Plot (d) is a color contour map projection showing the difference between CESM and GPCP .....	29
Figure 3: Absolute magnitude (in color) and the vector field is the tropical surface wind stress ( $\text{N m}^{-2}$ ) and direction with annual means (a) and boreal summer (b).....	30
Figure 4: Meridional transect from $0^\circ$ to $50^\circ\text{N}$ with mean zonal diabatic Heating ( $\text{K day}^{-1}$ ) over longitudinal bands $80^\circ$ to $90^\circ$ . Vectors are omega ( $\text{Pa day}^{-1}$ ) and have been scaled by $10^4$ to highlight vertical velocity .....	32
Figure 5: Regular-Plateau simulation, illustrating annual mean sea-level pressures (a) and boreal summer means (b) in milibars .....	33

Figure	Page
Figure 6: The descriptions for this plot are the same as figure caption 4, instead we have modern CAM4 simulations: No-Plateau (a), Half-Plateau (b), Himalayan-Wall (c) and Double-Plateau (d).....	34
Figure 7: JJA summer months divergence of wind at 100 mb pressure level were calculated using ncl divergence plotting tool. Divergence is scaled by multiplying units by $10^6$ (s-1) and vector magnitudes were plotted to show direction of wind. ....	36
Figure 8: The description for this plot is the same for figure caption 7. Plots a, b, e and f represents our perturbed simulations while plots c, d, g, and h are anomaly plots (test-control). ....	37
Figure 9: Precipitation rates of our four sensitivity test cases are plotted (a-d) and precipitation anomaly plots are plotted (e-f) as test-control. ....	40
Figure 10: Global mean integrated moisture flux from 1000 to 700 mb pressure levels during boreal summer. Vectors represent wind magnitudes and directions .....	42
Figure 11: The same description for figure caption 11 is used for this figure, with plots a-d as our anomaly plots .....	43
Figure 12: Global transient integrated moisture flux from 1000 to 700 mb pressure levels of JJA summer months is plotted on a color contour map with vector magnitudes plotted to show wind direction. ....	44
Figure 13: The same description for figure caption 13 is used for this figure, with plots a-d as our anomaly plots .....	45

Figure	Page
Figure 14: Global precipitation rates of control case with annual (a), JJA months (b) and DJF months plotted.....	46
Figure 15: Anomaly plots of global precipitation rates with JJA months as plots a-d and DJF months as plots e-h. ....	48
Figure 16: Regular-Plateau simulation showing extended seasonal cumulative precipitation rates ( $\text{mm day}^{-1}$ ) normalized and dived by annual cumulative precipitation rates ( $\text{mm day}^{-1}$ ) to show percentage of precipitation occurring seasonally. Areas highlighted are regimes with precipitation rates above $3 \text{ mm day}^{-1}$ . Extended months are MJJAS for NH months (plotted from $0^{\circ}$ - $90^{\circ}\text{N}$ ) and NDJFM for SH months (plotted from $0^{\circ}$ - $90^{\circ}\text{S}$ ). Individual square boxes highlight each monsoon areas. ....	51
Figure 17: This figure has the same description for figure caption 17. Highlighting our sensitivity cases No-Plateau (a), Half-Plateau (b), Himalayan-Wall (c) and Double-Plateau (d).....	52
Figure 18: Anomaly plots of CAM 5 No-Plateau and Double-Plateau simulations for global precipitation rates are plotted for JJA months (a-b) and DJF months (c-d.) .....	54
Figure 19: Annual surface temperature (a) and annual sea surface temperature (b) are plotted against percent plateau height with 0% as No-Plateau, 50% as Half-Plateau, 100% as Regular-Plateau and 200% as Double-Plateau. A fitted linear regression with and $R^2$ of 0.978 for ST Land and 0.988 for SST was taken to present how surface temperature responds to large orographic perturbation. ....	60



## ABSTRACT

Acosta, R. Paul, M.S., Purdue University, December 2013. The Influence of the Tibetan Plateau Elevation on the Global and Asian Monsoons. Major Professor: Matthew Huber.

It has been long hypothesized that large-scale topographic changes, such as the surface uplift of the Tibetan Plateau, impacts the development of the South Asian and East Asian monsoons and influences other monsoon regions. However, recent modeling has shown that spatial distribution of the global monsoon, which includes the South Asian and East Asian monsoons is largely unaffected by the elevation of the plateau. In this study, we present results from a series of modern day simulations using CESM1.0 in a mixed-layer (slab ocean) configuration. The Tibetan Plateau height is varied from double that of the modern maximum plateau elevation ( $\sim 9000$  m), down to near sea level elevation ( $\sim 10$  m).

Overall we find that the Asian monsoon system exists regardless of the plateau's elevation but its impact on Asia's hydrological system is undeniable. Specifically, reducing plateau elevation increases precipitation rates over Southern Asia and behind the plateau, but decreases orographic precipitation. In addition, when we remove the Tibetan Plateau, diabatic heating produced over the Himalayan Mountains and Tibetan Plateau disappears, and as a result, the integrated mean eddy moisture flux over

Southern Asia is reduced. In contrast, our double topography simulation shows a decrease in precipitation over Southern and Eastern Asia, but an increase in orographic precipitation. Furthermore, we see an increase in diabatic heating in our double plateau simulation, which contributes to an increase in mean integrated eddy moisture flux over Southern Asia. Our study suggests that diabatic heating produced by the plateau is an important mechanism that draws moisture over Asia, while removing the plateau reduces orographic precipitation and redistributes moisture over Southern Asia and further inland.

In general, global surface temperature decreases linearly as we increase the Tibetan Plateau's elevation. However, using a monsoon index based on the ratio of summer precipitation to annual precipitation, we show that the distribution of the global monsoon does not change substantially and the plateau's impact on the global circulation is relatively weak.

## 1. INTRODUCTION

Today, the Tibetan Plateau is the highest plateau on Earth, encompassing over 2.5 million km<sup>2</sup>, with an average elevation exceeding 4.5 km (Fig. 1a) (Harris, 2006). The history of the Tibetan Plateau's upward and outward growth remains controversial (Crowley and Burke, 1998; Volkmer et al., 2007). It is conventionally believed that the cause of uplift was due to the collision of the Indian subcontinent to the Eurasian continent. However, a combination of evidence from Ocean Drilling Project cores, and various sediment deposits suggest that Tibet was uplifted before the Indian subcontinent collided (Molnar et al., 2010). There are several competing hypothesis on how the unusual height of the Tibetan Plateau came to be: underthrusting of India into Asia; delayed continental underplating; continental injection; distributed shortening and continental extrusion (Harrison, Copeland, Kidd, & Yin, 1992). Nonetheless, this collision started ~50 Mya and continues today (Ruddiman, 1998; Yin and Harrison 2000; Kapp et al. 2003; Volkmer et al. 2007; Molnar et al. 2010). The result of such uplift contributes to direct and indirect impacts on the atmospheric circulation (Kutzbach et al., 1989). On longer time scales, its been proposed that the uplift of the Himalayas, Tibetan Plateau and Western Cordillera of North America fundamentally altered the pattern of atmospheric circulation in the Northern Hemisphere (Manabe and Terpstra, 1974;

Kutzbach et al., 1989; Molnar and England, 1990; Ramstein et al. 1997; Hay et al., 2002; Champagnac et al., 2012)

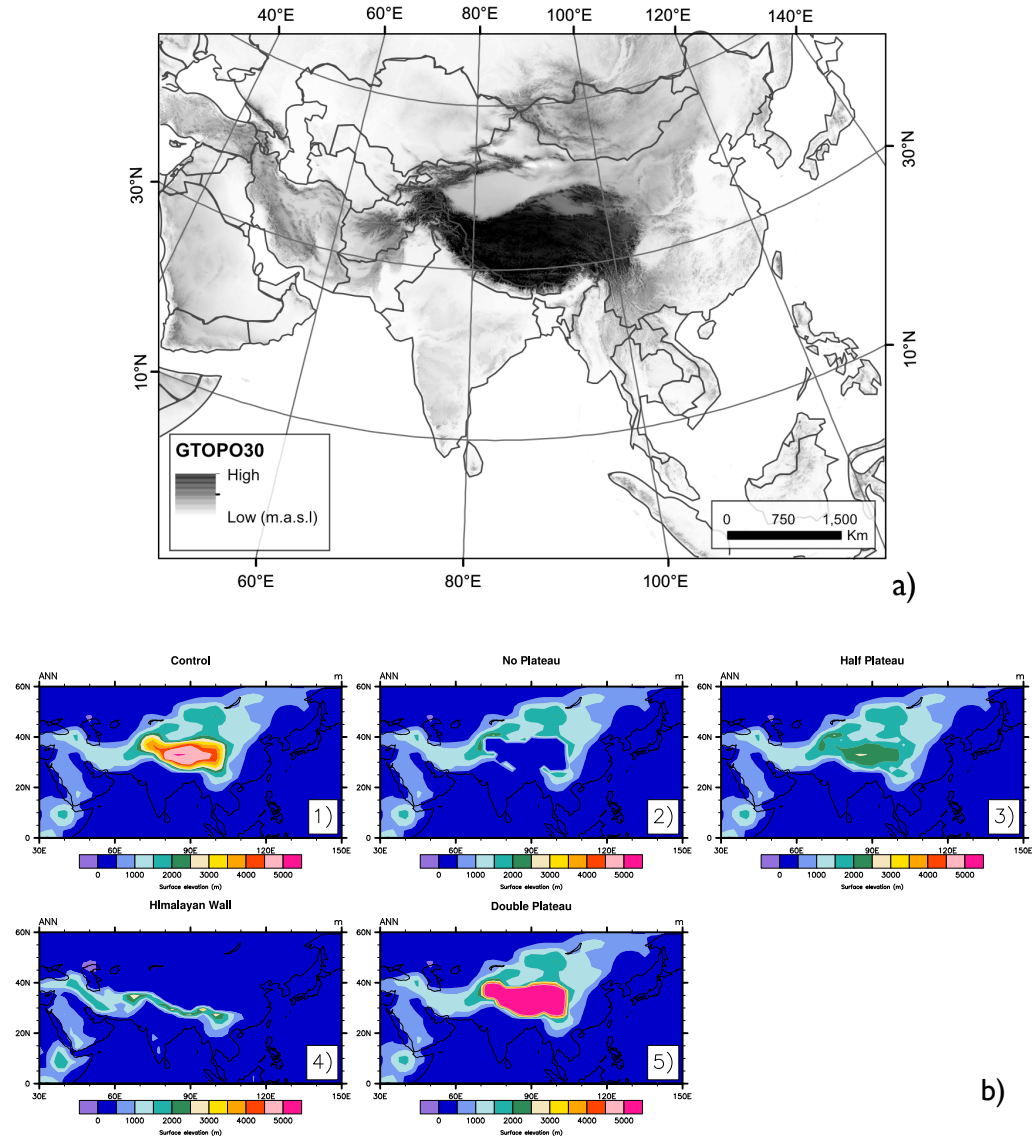


Figure 1: Displays the full extent of Tibetan Plateau, on a Lambert Conformal Conic projection with dark color as higher elevation (a). This image was from USGS GTOPO 30, assembled using ARC GIS by Robin Bloomdin. Image b, illustrates all of our topographic configurations: Control, No-Plateau, Half-Plateau, Double-Plateau and Himalayan-Wall.

In general, orography is thought to be a primary driver of monsoons.

Consequently, because Asia possesses the largest plateau topography, the Asian Summer Monsoon (AM) is the most studied monsoon circulation today (Holton, 2004) however the effects of Tibetan Plateau on the AM is currently in debate (Qiu, 2013). In addition, the evolution of the AM is intrinsically linked to the climate of the Asian continent, and its implication on society is one of the primary drivers for studying the monsoon.

Understanding its distribution, onset and strength is directly linked to the evolution of the Himalayan-Tibet uplift (Ruddiman and Kutzbach, 1989; Yanai and Li, 1994; Ruddiman, 1998).

In addition, the AM is part of a network of monsoon systems known as the global monsoon system. Where the extent of the global monsoon reaches large sections of the oceans and affects almost all of the continents except Antarctica. It is an important hydrologic system that directly influences natural disasters such as drought and floods, and also agricultural instability. Trenberth et al. (2000) first introduced the concept of the “global monsoon” as a global-scale seasonal overturning of the atmosphere, associated with seasonal variation in precipitation regimes. In addition, the global monsoon system is associated with seasonal periodic fluctuations, moving from the equatorial region and shifting poleward. These seasonal shifts of the global monsoon are intertwined with movements of the Intertropical Convergence Zone (ITCZ) (Chao, 2000; Zhang and Wang, 2008; Wang, 2009). As mentioned before, within the global monsoon system, are networks of regional monsoon systems that exist during Northern or Southern

Hemisphere summer months. The dominant monsoon systems are the Asian, Australian, African and the North and South American monsoon systems.

The monsoon was first discovered by Edward Halley during the 1700's, when he hypothesized that the main driver of monsoon systems is a strong thermal contrast between land and sea (Halley, 1686). Even today, many associate the onset of monsoon system such as SAM as part of a planetary-scale sea breeze that occurs between the Indian Ocean and the Asian continent (Zhang and Wang, 2008; Wu et al., 2012). Over the past decades, sensitivity of monsoon systems to topographical changes has been extensively explored and the majority of the scientific community focuses on the evolution of the SAM. Such scientific debate involves the controversial importance of the Tibetan Plateau acting as a heat source (Boos and Kuang, 2010; Huber and Goldner, 2012; Wu et al. 2012; Boos and Kuang, 2013; Chen et al., in review).

However, it is important to point out that modeling studies such as Bordoni and Schneider (2008) have shown the existence of the monsoon onset without presence of an inhomogeneous body such as continents. Bordoni and Schneider (2008) used an aquaplanet General Circulation Model (GCM) and concluded that the onset of the monsoon or poleward shift by the ITCZ, only requires changes in solar insolation (seasonal variation), and strong eddy momentum flux controlled by thermal inertia which contributes to the excess production of eddies and tropical meridional overturning. Nonetheless, it is important to study the effects of orography on individual monsoons because the presence of large topography such as Tibetan Plateau on the

Asian continent does alter the dimensions of the Asian Monsoon system and perhaps the strength of its precipitation.

The debate over the importance of the Tibetan Plateau as a heat source for the Asian monsoon was reignited Boos and Kaung (2010), when they presented results suggesting that the dominant thermal forcing that initiates the SAM is not the Tibetan Plateau. Instead their study suggested that the Himalayan Mountains acting as a barrier that prevents cold extratropical air from entering Southern Asia, and heating produced by Southern Asia are the only required features to produce the SAM. However, several opposing simulation studies have shown that inland migration of the SAM requires heating over the plateau (Huber and Goldner, 2011, Wu et al., 2012; and Chen et al, in revision) (see section 2.3 for more details). One of the goals of this study is to explore and quantify the importance of the Tibetan Plateau on the SAM.

Huber and Goldner (2011) have shown the robustness of the global and Asian monsoon systems throughout the Eocene. However, they emphasized that the drastic changes in boundary conditions, such as continent configuration, and a warmer climate system may have also affected the strength and distribution of the global monsoon system. They further hypothesize that in a colder climate system with a more enhanced temperature gradient, the response of the global and specifically the Asian monsoon system to Tibetan Plateau's elevation would present a different result. One motivation for this study is to build upon the questions presented by Huber and Goldner (2011) and better constrain the implications of Tibetan Plateau on the global and Asian monsoon. This thesis illustrates a more simplified sensitivity study on the monsoon systems by

only altering the Tibetan Plateau in modern boundary conditions. We used the same GCM model as Boos and Kuang (2010), Huber and Goldner (2011), and Chen et al. (in review), but strictly used slab ocean atmospheric model (see Section 3). Furthermore, we test the robustness of our results by using two different atmospheric models CESM1 CAM4 and the more up-to-date version CAM5.

The structure of this paper is as follow: section 2 reviews detailed information about the physical effects of topography on climate, background information about individual monsoon regions, and a literature review on modeling studies conducted regarding the Tibetan Plateau. Section 3 will discuss the methodology, and reasoning behind our experiments. It will discuss model framework, experimental design, and specific monsoon indices. Section 4 presents our results on model-data product comparison, and our topographic sensitivity studies using two different atmospheric models. Section 5, we discuss the impact of my results in the context of previous work, as well as the robustness of the results achieved in this study. Lastly, section 6 will conclude and describe necessary future work and the implications of my results.



## 2. BACKGROUND

The following sections will introduce (2.1) the basic concepts describing how large-scale topography influence climate and weather, (2.2) summarizes individual monsoon systems, specifically the Asian summer monsoon, which consist of South Asian Monsoon (SAM), the East Asian Monsoon (EAM), the Australian Monsoon (AM), the West African Monsoon (WAM), the North American Monsoon (NAM), also referred to as the south American monsoon and the South American Monsoon Systems (SAMS). The last section (2.3) reviews the literature regarding the Tibetan Plateau and how it influence the Asian and global monsoon.

### 2.1 Mountains and their influence on climate

On geologic time scales, orography has been proposed to profoundly affect the circulation of the atmosphere (Molnar and England, 1990; Hay et al., 2002; Molnar et al., 2010). The physical presence of mountains and plateaus strongly alter zonal circulation, and can dictate regional climate variation. It has been estimated that mountains or high plateaus occupy approximately 20% of the Earth's land surface. In addition, approximately 10-26% of the world's population lives on or within 50 km of mountains (Oliver, 2005), therefore it is important to understand orogenic influence on climates systems. A more extensive explanation on how elevated topography effect climate are

described in many meteorological texts Manabe and Terpstra, (1974); Kutzbach et al., (1992); Wallace and Hobbs, (2006), and Holton, (2004), for the purpose of this study, we have reviewed some primary effects of orography on large-scale climate.

First, elevated regions pose as a physical obstacle that deflects airflows. Airflow must either overcome the height of the mountain or move around it. Second, as flows rise above mountain ranges, their spin dynamics is drastically enhanced. Spin dynamics can be explained through conservation of potential vorticity (PV), which refers to a parcel's circular flow about its origin (vorticity); where the static stability (the ratio of the absolute vorticity and the depth of vortex) of the flow is reduced between the boundary layer and the elevated regions, and then expanded as it moves past such regions (Martin, 2006). In addition, the Coriolis force simultaneously influences this process as it moves away from the equator. To give clarity to the subject, imagine a column of air parcel confined between two surfaces with equal potential temperature (isentropic) moving as a westerly flow across Eurasia. As the flow crosses over the Tibetan Plateau the depth of the column impinged, and due to conservation of potential vorticity, the air parcel's absolute vorticity must simultaneously increase. As the column moves past the elevated region, static stability is reduced and the air column begins to stretch. Characteristically, westerly wind currents encountering an elevated region, results in adiabatic warming (warming due to expansion and contraction of volume) of the air near the leeward surface and produces wave like climatological patterns.

In Eurasia, plateaus like the Tibet are known to be a source of sensible heat for the atmosphere. During summer radiative heating warms the plateau's surface and

along with its overlying atmosphere. During winter as other factors such as snow and shorter solar insolation contribute to the cooling of the surrounding atmosphere above the plateau. Such cooling and warming of air parcels around elevated regions develops relatively strong density contrasts and produces high and low pressure systems. These pressure systems create strong rising and sinking motions which then produce strong horizontal inflow and outflow of wind, respectively (Abe, Yasunari, & Kitoh, 2004; Kitoh, 2002; Kutzbach et al., 1989; Prell & Kutzbach, 1992; Webster & Chou, 1980). For example, because of the combination of wind reversals due to seasonal temperature gradients, and the barrier-like characteristic of Himalayan-Tibetan mountain range, the climatology of Southern Asia consist of wet summers and dry winters. In addition, as air parcels rise over topography, they expand and allow condensation to occur. As water molecules change their phase, they release latent heat and further accelerate their rising. Another way to produce latent heat is the constant evaporation of moisture over a warm ocean surface. This heating becomes important when considering the creation of convective systems.

## 2.2 Overview of Monsoon Systems

The English term “monsoon” originated from the Portuguese word “moncoa” and from the Arabic word “mausim” which means season (Oliver, 2005). The formation of a monsoon has implications on agricultural, economical, and social importance. Therefore, it is crucial to understand its distribution in regional and global scales, and further explore the mechanisms behind its formation. In general, monsoon onset begins

with a strong thermal gradient imbalance, causing typical wind direction to reverse by at least 120° shift in direction (Oliver, 2005). Conditions such as low tropospheric moist entropy and a warm upper-level temperature, will enhance convection of lower-tropospheric water vapor (Molnar and Emanuel, 1999; Yanai and Li, 1994; Plumb, 2005). Furthermore, the effects of tectonically induced orographic changes are also important factors when considering monsoon formation and long-term evolution (Raymo and Ruddiman, 1992).

The AM consists of the East Asian Monsoon (EAM) that brings heavy rain in late spring/early summer and the South Asian Monsoon (SAM) that usually marks the onset of summer precipitation in India and China. The SAM is a tropical monsoon in which rain falls almost entirely as part of ITCZ migrating poleward from the equator (Chao, 2000; Molnar et al., 2010). It was believed that the diabatic heating of the atmosphere caused by the Tibetan Plateau was the main mechanism for the SAM (Reiter, 1968; Yanai and Li, 1994; Wu et al., 2012). However recent studies have shown that majority of the heating occurs at the northern part of India and the elevated Himalayan mainly acts as a barrier that prevent cold and dry extratropical air from ventilating the warm and moist tropics (Boos and Kuang, 2010; 2013). Studies using climate models do not explicitly disqualify the importance of the Tibetan Plateau in the SAM (Chakraborty et al., 2006; Wang et al., 2008; Huber and Goldner, 2012; Wu et al., 2012; Chen et al., in review). These are further reviewed in the following literature review section.

The EAM is distinctly different from the SAM, due to its extratropical nature, where precipitation and winds are associated with frontal systems and the jet stream

(Kitoh, 2002 and 2004). Here, the main mechanism involves the subtropical jet passing south of Tibet when wind speeds are highest. Heavy precipitation usually starts early summer, in the sea of the Philippine Sea and largely effect regions near northern China and Japan. It is believed that the presence of the Tibetan Plateau such as Tibet in combination with a high speed jet stream, produces strong zonal gradients in velocity which then induce divergent flows (see static stability in section 2.1) that accelerates the onset of the mei-yu (China) and baiu (Japan) rain band (Nigam, et al. 1986 and 1988; Kitoh, 2002 and 2004; Molnar et al., 2010).

The Australian Monsoon and Maritime Continent monsoon occurs in austral summer (December-March). These monsoon circulation do not appear primarily driven by land-ocean temperature contrast, (Hendon and Brant, 1990; Li et al., 2012) instead the source of moisture primarily comes from northwesterly flow of humid maritime air during winter solstice and the occurrence of southeast trade winds in the Southern Hemisphere. It is common for the East Asian winter monsoon and the North Australian summer monsoon occurs simultaneously, and are considered inherently linked, with the winter Asian monsoon providing a “pressure push” for wind crossing the equator to contribute to the Australian summer monsoon (itself providing a “thermal pull”) (An, 2000)

The WAM originates from the tropical Atlantic Ocean, extending over the sub-Saharan dessert and as far east as Ethiopia. It is a product of wind reversal from southwesterlies in the summer and northeasterlies in the winter (Oliver, 2005). The rainfall seasonal cycle over the western coast of Africa begins with greatest amount of

precipitation during August, when the ITCZ is located at the northernmost latitude (Sultan and Janicot, 2003). In addition, two rainy seasons can be observed on the eastern side of Africa: one that occurs during March-May, which is known as “the long rain” and another from October-November “the short rain”. These rainy periods fall between the two African monsoon circulations (Oliver, 2005). The WAM in addition to African Easterly Waves ultimately dictates general circulation around North Africa and also influence hurricanes in the Atlantic (Hopsch et al., 2010; Stein et al., 2011).

The North American Monsoon system, also known as the southwest United States monsoon, the Mexican monsoon or the Arizona monsoon and primarily occurs during northern hemisphere summer, and begins with an extremely dry June which proceeds to a rainy July and continues until mid-September. It is a lesser and small versions of its northern hemisphere counter part (SAM), but nonetheless an important regional hydrologic system that influences local climatology. Its onset is generally characterized by substantial change in surface zonal wind from a dominant easterly in January to a reversed westerly in July (Oliver, 2005). Furthermore, decrease in mid latitude transient synoptic in United States and northern Mexico are usually associated with the onset of the NAMS (Higgins, Yao, & Wang, 1997). It is mainly believed that the combination of seasonal warmth from the low lands of the lower Colorado River Valley, coastal lowlands of Sonora and Sinaloa, and elevated areas are Colorado Plateau, Rocky Mountains, Basin and Range province and Sierra Nevada mountain range produces strong surface temperature heating. With this heating, and introduction of atmospheric moisture supplied by nearby maritime sources such as the Bermuda and/or Gulf of

Mexico creates a system that is conducive to the formation of a monsoon circulation (Adams and Comrie, 1997).

The South American continent was first considered to be a monsoonless continent. The persistent upwelling system, off the west coast of South America shows that in average, wind flow over this region is unidirectional year round. It was believed that South America lacked the required seasonal wind-reversal for monsoon formation. However, severe thunderstorms and large-scale precipitation events were frequently recorded over the Altiplano during SH summer months, which caused the scientific community to question if South America was actually a monsoonless continent. Later on, it was hypothesized that the Altiplano Plateau (Rao and Erdogan, 1989) and the Amazon (Zhou and Lau, 1998), both acted as the driving heat source that supplied substantial diabatic heating and corresponding vertical motions for the observed convective systems. This was later identified as the South American Monsoon System (SAMS). Zhou and Lau (1998), summarized the onset of SAMS as a perturbation due to thermal gradient between the subtropical highlands along 20° S of the equator and the surrounding ocean. Simulations by Lenters and Cook, (1995) have shown that Amazonian precipitations during summer monsoon months were largely due to land sea thermal contrast from topographic heating. They also showed that precipitation in the Andes becomes absent when topography is removed.

Each monsoon system is characterized by differences in spatial distribution, duration and magnitude. Additionally, the recipes for initialization of a monsoon system are still highly debated, but common features persist in each monsoon system. The

overwhelming effects of ocean-land temperature gradient, and perturbations due to large scale topography are important mechanisms, although not required (Bordoni, 2008), that influence individual monsoon systems.

### 2.3 Literature Review on Tibetan Plateau simulations

Since the 1960's, the explorations of orographic effects on climate have been performed using numerical models (Manabe and Terpstra, 1974). Since this thesis focuses on monsoon systems through simulations using global climate models, we believe it is important to revisit past studies that have explored monsoon dynamics using similar methodologies. Thus, we revisit influential works by Mintz (1965); Manabe and Terpstra (1974), Ruddiman and Kutzbach (1989), Prell and Ruddiman (1992), Ramstein et al. (1997), Chakraborty et al. (2006), Boos and Kaung (2010), Huber and Goldner (2011), Wu et al. (2012), and Chen et al. (in revision).

Mintz pioneered the construction of a successful global model with realistic orography where he first compared a with-mountain and without-mountain simulations (Eagleson, 2010). His comparisons suggested that the Tibetan plateau is responsible for the maintenance of the intense planetary waves during winter. Manabe and Terpstra (1974), used the Geophysical Fluid Dynamics Laboratory (GFDL) general circulation model (GCM) with hydrologic cycle, to simulate the implications of topographical features located in Asian and the American continent.



In their study, they used the same boundary conditions as Mintz (1974) to demonstrate the distribution of stationary eddy kinetic energy ( $K_E^{TS}$ ) defined by

$$K_E^{TS} = \frac{1}{2} [\overline{u^2} + \overline{v^2}] \quad (1.1)$$

and transient eddy kinetic energy ( $K_E^{TE}$ ) define by

$$K_E^{TE} = \frac{1}{2} [\overline{u'^2} + \overline{v'^2}] \quad (1.2)$$

where  $u$  and  $v$  are denoted as zonal and meridional component of wind,  $\overline{(\ )}$  indicate zonal mean operators and  $(\ )'$  denote the deviations from time-mean. They found that topography of the Earth's surface significantly alters the distribution of the eddy kinetic energy between  $K_E^{TS}$ , and  $K_E^{TE}$  disturbances, such that angular momentum are predominantly influenced by stationary eddies, while heat, and moisture fluxes are more influence by transient eddies.

Ruddiman and Kutzbach (1989) illustrated the importance of plateau uplift in the Northern hemisphere using a Community Climate Model (CCM). In this study they improved upon previous works by using a model with an improved dynamical core, and radiative and convective processes (Kutzbach et al., 1989). Their experimental design was a set of topographical configuration: no-mountain, half-mountain, and full-mountain over Southern Asia and the American West. This simulated the evolution of Earth's atmospheric circulation and climate response to mountain uplift. Ruddiman and Kutzbach (1989) showed that the magnitude of changes in spatial patterns of temperature and precipitation changes between cases no mountain, half-mountain and full-mountain is generally proportional to the relative amount of uplift between

experiments. With regards to Tibetan Plateau, they showed that uplift induces changes in summer circulation and produces deflection of airflow surrounding the Tibetan Plateau, and increased northeasterlies over Asia and Arabia, and further strengthening of the Asian monsoon system. The main limitation of Ruddiman and Kutzbach, (1989) is the lack of interactive ocean in the model, where they used fixed sea surface temperature. This deficiency prevented the ocean surface from adjusting and reacting to atmospheric perturbations.

Prell and Kutzbach (1992) continued such work using NCAR's CCM1, demonstrating large-scale forcing such as orography over Asian continent augmented by radiation (orbital) changes affects Indian Ocean summer monsoon circulation. They concluded that monsoon precipitation rates increases as elevation is increased. Where as removal of the Asian mountains produced weaker summer winds over Arabian Sea. Their half mountain simulation firmly establishes the southwesterlies, but is still weaker than regular mountain height. Broccoli and Manabe (1992), demonstrated that the introduction of large mountain ranges such as the Tibetan Plateau and the Rocky Mountains increased the likelihood of northern hemisphere aridity. They used GFDL climate model version, with experimental design consisting of No-mountains, with Mountains and a fixed soil moisture integration on a with mountains simulations. Broccoli and Manabe suggested that the existence of the Tibetan Plateau causes extensive dryness over central Asia, compared to the no mountain experiment. By utilizing band-pass filter (the anomaly of total eddy flux and stationary eddy flux) it is shown that no mountain simulations allow propagation of more storm tracks toward

central Asia. Moving forward, Ramstein et al. (1997), used an improved model (coupled slab ocean and atmospheric GCM), and were the first authors to use realistic paleogeographical reconstructions of three time periods: Oligocene, Miocene, present day. With these experiments they concluded that the Himalayan mountain range limits the outflow of cold air toward the Indian subcontinent during winter. In addition, the Himalayan and Tibetan uplifts strengthen the winter ridge producing desertification of central Asia and regions of Middle East. Zhisheng et al. (2001) used the combination of proxy record from the Miocene and paleo-reconstruction methods via climate models to study the effects of the Tibetan plateau on the Asian monsoon. Their methodology consisted of four step-wise increase of the plateau height, going from 1,000 to 4,500 meters. They concluded that introduction of 2700 meter elevation above is substantial enough to induce strong winter and summer monsoon over Asia.

Kitoh (2002 and 2004) tackled the problem of Asian monsoon sensitivity to mountain uplift by applying a coupled atmosphere and ocean GCM. In their study they simulated a suite of mountain elevation going from 0% to 140% in increments of 20%. They concluded that prior to the existence of a 100% plateau the baiu rain band, which is an indicator of the East Asian Monsoon onset, did not exist. In addition, the strong thermal contrast due to the deep heat source found in the South and Southeast Asian continent already exist prior to the full uplift of the plateau. They alluded to the conclusion that the Tibetan Plateau affect zonal wind fields and modifies the summer monsoon circulation.

Chakraborty et al. (2006) studied the onset of the monsoon by perturbing orography not only in the Indian sub-continent but also, North and South America, Africa and several variation of the Himalayas. They used a global atmospheric GCM produced by National Center for Environmental Prediction (NCEP), with 5-yr simulations size. From this, Chakraborty et al. (2006), accompanied by Broccoli and Manabe (1992), Kitoh (2003), arrived at the same conclusion that the mid-latitude precipitation maximum in spring is associated with the introduction of high topography such as the Tibetan Plateau. They also concluded that the removal of the West portion of Himalayas considerably set the onset of monsoon later than removing the east portion and that the East Himalayas do not affect monsoon rainfall. Lastly, the removal of the African orography increases the moisture convergence of the Indo-Asian monsoon.

Boos and Kaung (2010) challenge the purpose of the Tibetan Plateau as the heat source for the large-scale temperature gradient is thought to invoke the South Asian Monsoon. Using both observational products in addition to modern fixed SST simulation from NCAR's CCSM (CAM 3), they concluded that by keeping the Himalayan Mountains and eliminating the Tibetan Plateau major thermal forcing is located south of Himalayas. Further suggesting that the plateau has minor effects on precipitation, and lower troposphere winds but does matter for eastern portion of the plateau. While Huber and Goldner (2011), emphasize the importance of the Tibetan uplift to the Indo-Asian Monsoon using a fully coupled model with Eocene epoch configuration (NCAR's CCSM3, CAM3). They argued that orographic uplift of the Plateau allows poleward redistribution of diabatic heating, which is not seen in simulations without topography. They further

illustrated this phenomena as cause of reduce precipitation rate north of the Tibetan Plateau and showed an increase around central Asia in an Eocene world. Regarding the global monsoon, Huber and Goldner suggested that the Global Monsoon precipitation was largely unaltered with or without the elevated plateau.

Wu et al. (2012) supported the importance of the large mountain range in the Asian summer monsoon. They used the Spectral Atmospheric Model of IAP/LASG (SAMIL) developed at State Key Laboratory of Numerical Modeling for atmospheric Science and Geophysical Fluid Dynamics. Their experimental design consisted of several Asian topography configurations including modification of the Iran Plateau. In addition, three compared simulations with surface sensible heating versus removed surface sensible heating over designated plateaus were used to measure the importance of the land-sea thermal gradient produced by topography. Such experiments demonstrated the importance of the thermal forcing induced by the Asian mountain ranges and concluded that heating resulted in further inland precipitation, strengthening the ASM. Wu et al, (2012) also explored orography lifting over the Himalayan/Tibetan Plateau and concluded that with Boos and Kuang (2010) Himalayan wall only force parcels to move around the wall, while the combination of the Himalayan wall and the Tibetan Plateau induced a climbing flow that produces monsoon cloud and precipitation. They suggested that climbing flow occurs due to the diabatic heating over the Tibetan Plateau.

Boos and Kuang (2013) proposed a counter argument, utilizing CESM1.0.4 where the surface sensible heat flux (SHFLX) over the Himalayan Wall and over the Indian subcontinent was set to zero, similar to Wu et al. (2012) methodology. Here they

showed that the prevention of SHFLX over the non-elevated region posed a stronger reduction of precipitation in the low-level monsoon westerlies than the shut off of Himalayan Wall SHFLX. Further suggesting that the SAM is more sensitive to the suppression of SHFLX of the non-elevated region.

In the most recent findings, Chen et al. (in review) revisited the implication of the barrier effect using the fully coupled AGCM, CESM1. Their simulations yielded similar general results with full Tibetan Plateau and No topography, to previous Tibetan simulation (mentioned above). For example they showed the necessity of the plateau for the production of the East Asian Monsoon and precipitation over East Asia (Kitoh, 2003; Boos and Kuang, 2010; Wu et al., 2012), and excess poleward drying with the plateau (Broccoli and Manabe, 1992; Huber and Goldner, 2011; Wu et al., 2012). However, they concluded that convection over non-elevated regions is much weaker in full plateau simulation suggesting that the barrier “blocking” and diabatic heating over non-elevated regions cannot fully account for the existence of the SAM. This further alludes to questioning the true purpose of the plateau and how it affects Asia’s climate and the Asian monsoon circulation and perhaps the global monsoon circulation.

### 3. METHODOLOGY

We produced a suite of global climate simulations using the National Center for Atmospheric Research (NCAR) Community Earth System Model version 1.0 (CESM 1.0) described in (Neale et al., 2013; Gent et al., 2011a; Bitz et al., 2012). We ran equilibrium climate simulations in slab-ocean mode and applied two types of atmospheric components. The CESM1.0 slab ocean configuration (E case) is fully equipped with a mixed layer depth. In addition, it is capable of thermodynamically responding to the atmosphere (Danabasoglu and Gent, 2009). Although slab ocean configurations inherently do not resolve ocean dynamics, it has been shown by Goldner et al. (2011) and Goldner et al. (2013) that there are no substantial ocean circulation differences between the models. We use this configuration because it is computationally inexpensive, it has an appropriate interactive surface temperature exchange with the atmosphere, and it can produce sufficient thermal gradients required for monsoon onset (Ramstein et al., 1997).

Using a finite volume dynamical core with calculations carried out on a grid with a spacing of  $\sim 1.9^\circ \times 2.5^\circ$ , we explored global and Asian monsoon circulation using the Community Atmospheric Model 4 (CAM4) with modern boundary conditions. The CAM4 is the sixth generation Atmospheric General Circulation Model (AGCM) built by the

Atmospheric Model Working Group. This version contains fully integrated chemistry, a finite volume scheme as a defaulted dynamical core (Hurrell et al., 2012). It has atmospheric dynamics that includes physics and flux such as radiation tendencies, convection, large-scale precipitation, boundary-layer diffusion, and resolves at a horizontal resolution of  $1^\circ$  and 26 vertical levels (Hurrell et al., 2012). It uses the Zhang and McFarlane (1995) simplified deep convection scheme. The primary improvements in this version of the model are improved spatial patterns of precipitation, reduction of inconsistent stratiform clouds and reduction of wind biases such as tropical easterly, subtropical westerly and excessive Southern Hemisphere mid-latitude jet stream. Modern experiments were run for more than 90 plus years, while pre-industrial simulations ran for more than 60 years (Table 1). Our results were averaged over the last 20 years of each simulation. Pre-industrial cases have 1850 boundary conditions, and modern cases have boundary conditions set to 20<sup>th</sup> century. Major differences between the two settings are the data input used to initiate each runs such as concentrations of greenhouse gasses used by the atmosphere model and the land cover usage.

Additionally, we tested how sensitive our results were to the new microphysical parameterization employed in the latest version of CAM (CAM5). This version has a new interactive, indirect aerosol parameterization in cloud formation and a more realistic boundary layer (Neale et al., 2013) These changes in aerosol physics influence the formation of cloud condensation nuclei (CCN), and the sensitivity of cloud droplets and ice crystals to radiative forcing (Song et al., 2012). However, the CAM5 configuration



uses similar dynamics as CAM4, although with different diabatic heating processes (Hurrell et al., 2012; Meehl et al., 2013). It is important to point out that model-to-model comparison between CAM5 and CAM4 shown an equilibrium and transient climate response substantially warmer in CAM5 (Meehl et al., 2013). Where equilibrium runs with double CO<sub>2</sub> concentration in CAM5 produce a global average surface air temperature of 4.10°C, CAM4 produces a 3.20°C increase (Gettelman et al., 2012). These changes are important to consider as we explore the global and Asian monsoon circulation.

### 3.1 Experiment Design

In this study we isolate the changes in topography of the Tibetan Plateau to fully explore its effect on the global and Asian monsoons (Fig. 1a). Four Tibetan Plateau topographic configurations were used in this study: a reduced plateau with topographic elevation near sea level (No-Plateau) (Fig. 1b2), a half modern height (Half-Plateau) (Fig. 1b3), a modern elevation (Regular-Plateau) (Fig. 1b1) and a double Tibetan Plateau (Double-Plateau) (Fig. 1a5). These are not intended to represent the geologic evolution of the plateau, but to act as a series of sensitivity test to help isolate the sole contribution to changes in atmospheric circulation by the Tibetan Plateau. The double plateau case is especially unrealistic, but provides a good test of the linearity of the responses seen in our simulations with reduced elevation. We used NCAR Command Language (NCL) to produce all topographic modifications on the USGS-gtopo30 map. The No-Plateau was lowered to 100 m above sea level. Then we incrementally increased

the height of the plateau from half the modern Tibetan Plateau, with maximum height ~2400 meters above sea level, to modern plateau elevation ~4900 meters above sea level; and lastly we doubled the plateau elevation ~9000 meters. In addition, we ran slab ocean simulations with the Boos and Kuang (2010 and 2013) Himalayan-Wall configuration directly following his methodology (Boos and Kuang 2010 supplementary) (Fig. 1b4). Simulations with a modern plateau elevation were used as our control simulation and we compare all other configurations against it.

### 3.2 Monsoon Indices

There are numerous definitions of both the global monsoon and in many cases each of the commonly recognized regional monsoons. There are two categories of definitions of the monsoon that relate to deep-rooted differences in the hypothesized mechanism for the monsoon; the first relates primarily to the changes in wind fields and the second focuses primarily on the seasonality of precipitation. The explanation of how the monsoon forms also differ within the scientific community, for example the conventional mechanism for a monsoon is a planetary sea-land breeze driven by differences in temperature gradients through heating of continents and topography (Halley, 1686). A secondary mechanism is the shifting of the Intertropical Convergence Zone (ITZC) due to changes in seasonal surface pressure which brings in tropical trade winds poleward and that produces convective circulation (Trenberth et al., 2000; Wang, 2009). The most recent defined mechanism for the monsoon is caused by shifts in solar insolation from the equator toward the mid-latitude regions and in addition, eddy

moisture fluxes from the tropics (Bordoni and Schneider, 2008). These definitions are dynamically relevant and have been used to understand and infer the past history of the monsoon. Changes in prevailing winds present themselves in upwelling records Anderson et al. (2010), whereas changes in precipitation are recorded in paleo-precipitation proxy records (Greenwood, 1996).

Similar to Wang and Ding (2006) we characterize monsoon climate by a rainy summer and a dry winter and by annual reversal of prevailing surface winds. In this study, we will focus on locations mentioned in our background and choose to quantify monsoon distribution and strength based on the definition developed by Zhang and Wang (2008). For the NH summer monsoon, the months of May, June, July, August and September (MJJAS) are averaged. For the SH summer monsoon, the months of November, December, January, February and March (NDJFM) are averaged. Monsoon regions are herein defined by areas receiving more than 55% of their total annual rainfall during summer as well as having a minimum summer precipitation rate of 3 mm day<sup>1</sup> (Zhang and Wang, 2008).

### 3.3 Observed Precipitation

We evaluate the precipitation bias of our models by comparing our control run against observations average over period 1979-2009 from the Global Precipitation Climatology Project (GPCP) (<http://www.gewex.org/gpcp.html>). We used GPCP version 2.1 monthly precipitation converted to mm day<sup>1</sup>. This data set comprises of global 1° x

1° resolution precipitation derived from GOES, NOAA and Meteosat satellite observations and surface measurements. The GPCP data set was interpolated to 1.9° x 2.5° resolution to match our model resolution and we used a 30-year climatology from both GPCP and CESM1 for our comparison.

Table 1

<b>CAM4</b>				<b>CAM 5</b>	
<b>MOD</b>	<b>YRS</b>	<b>PRE-IND</b>	<b>YRS</b>	<b>PRE_IND</b>	<b>YRS</b>
No-Plateau	90+	No-Plateau	60+	No-Plateau	60+
Half-Plateau	90+	/	/	/	/
Full-Plateau	90+	Full-Plateau	60+	Full-Plateau	60+
Double-Plateau	90+	Double-Plateau	60+	Double-Plateau	60+
Boos-Wall	90+	/	/	/	/

## 4. RESULTS

This section will be subdivided into four main parts: (4.1) precipitation biases, (4.2) the influence of orographic perturbation regionally, (4.3) changes in global monsoon and global precipitation due to elevation change of the Tibetan Plateau, and (4.4) sensitivity to GCM version. In section 4.1 to understand our model's biases, we compared our modern CAM4 simulation against GPCP observational product. In section 4.2, we show the regional impact of changing the elevation of Tibetan Plateau. We explore physical and dynamical changes by looking at three main subsections: (4.2.1) diabatic heating over Asia, (4.2.2) divergence of wind and precipitation regimes over Asia, and (4.2.3) mean and transient integrated moisture transport. We then look at the global response (4.3). In section 4.3 we used the Monsoon Index mentioned in our methods section to understand monsoon distribution, and also looked at global precipitation regimes, comparing all four configurations. Our last sections will compare CAM4 and CAM5 and show how CAM5 responds to orographic changes.

### 4.1 Precipitation Biases

When comparing our control case to the GPCP data set, we can see that the spatial distribution of JJA precipitation is similar within reason (Fig. 2a and 2b). Overall precipitation trend in our zonal average plot (Fig. 2c) are nearly identical. However,

large discrepancies are seen near the equator ( $10^{\circ}\text{S}$ ). In particular, CESM1 CAM4 has a higher precipitation peak than GPCP, including precipitation rates found on the SH (Fig. 2c). Considering our anomaly plot (Fig. 2d), we observe that CAM4 has a larger JJA precipitation bias over the Himalayan Mountains, with a difference of  $\sim 20 \text{ mm day}^{-1}$  and the western section of India with a difference of  $\sim 8 \text{ mm day}^{-1}$ . In contrast, CAM4 has lower precipitation rates than GPCP over Bangladesh, northern section of South America, southern parts of Mexico and a large section of the Mid-Pacific Ocean, with precipitation rates over  $6 \text{ mm day}^{-1}$ . Furthermore, the split ITCZ produced by our simulation is well captured over the Central Pacific Ocean (Fig. 2d). Despite these biases the CESM performs better than previous versions of the model and several of the observed biases may be mediated by employing a coupled ocean-atmosphere version of the CESM (Meehl et al., 2011). However, our work is mainly for a theoretical purpose and should only be used as a useful framework to study and understand physical processes.

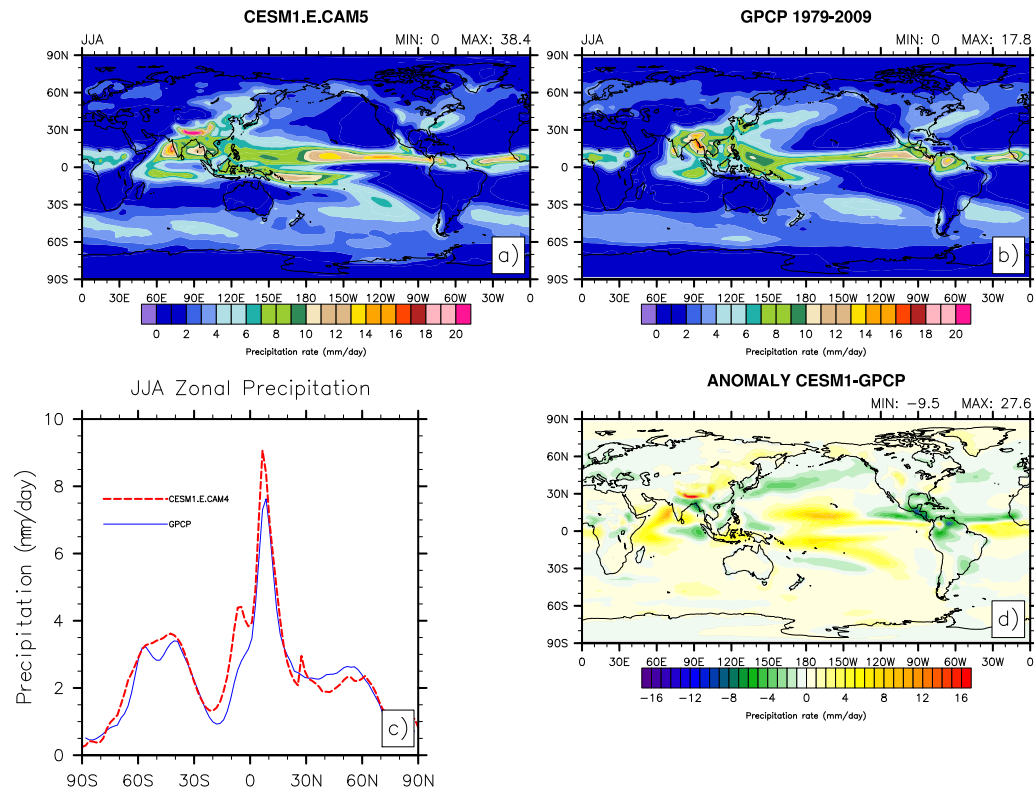


Figure 2: Global precipitation distribution of Modern CESM CAM4 and GPCP 1979-2009 are shown in plots (a and b). Where as plots c and d shows the comparisons between the two. Plot (c) is a meridional transect with mean zonal global precipitations. Plot (d) is a color contour map projection showing the difference between CESM and GPCP.

## 4.2 Influence of the Tibetan Plateau

Sections 4.2.1 – 4.2.3 will explore general circulation patterns over Asia and how it they are affected as the Tibetan Plateau is raised, lowered and removed. Section 4.2.4 will explore then talk about the barrier effect of the Himalayan wall.

### 4.2.1 Heating Over Asia

During Northern Hemisphere summer months, the Tibetan Plateau has always been considered a source of an anomalously high diabatic heating over the Asia. This

heating induces a large thermal difference between land and sea. This large thermal gradient produces a planetary scale sea-land breeze. This driving mechanism has been hypothesized to influence the poleward movement of the ITCZ (Wang, 2006), and the annually occurring easterly flow to move from the equator toward the Asia (Fig. 3). In this section we test this hypothesis and show the effects produced by this heating.

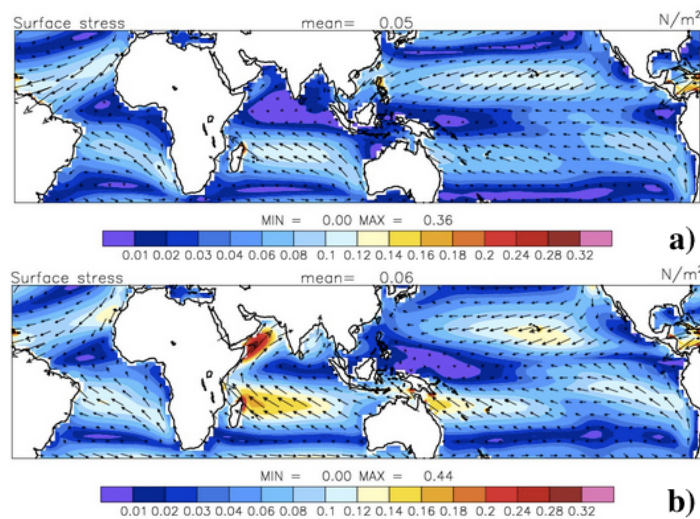


Figure 3: Absolute magnitude (in color) and the vector field is the tropical surface wind stress ( $Nm^{-2}$ ) and direction with annual means (a) and boreal summer (b).

In our simulations, diabatic heating was calculated by summing up the solar heating rate, longwave heating rate, vertical temperature diffusion and temperature tendencies. The shortwave heating rate is the total solar heating of the atmosphere over specified regions. The longwave heating rate is the heat gained from the emission of longwave radiation from the ground and the atmosphere. Temperature diffusion is the rate of energy transferred by conduction over time. The temperature tendency is defined as the local change of temperature that is equivalent to two horizontal



advection components, adiabatic temperature change due to vertical movement and diabatic heating. Temperature tendency includes heat released during phase change of water (latent heating) and a system's change in temperature due to heat exchange (sensible heating).

It can be seen in our control simulation that total annual diabatic heating over Tibet is minimal compared to during boreal summer (Fig. 4). During summer months this heating can be well above  $8 \text{ K day}^{-1}$  and extends its reach to higher levels of the atmosphere (above 250 mb or 12 km above sea level). We also see that heating over lower regions of the plateau, from  $0^\circ\text{N}$  to  $25^\circ\text{N}$ , is much greater during summer months. We also see that during the summer months, strong vertical motion (Fig. 4b) and lower surface pressure are seen over Asia. These phenomena have been observed and reproduced in other modeling work (Yanai and Wu, 2006) (Fig 5).

Comparisons between our five simulations show drastic differences in JJA diabatic heating over Asia (Fig 6). Here we show that even with the removal of high topography the Tibetan Plateau maintains its diabatic heating over the Indian subcontinent ( $4 \text{ Kday}^{-1}$ ) but removes all excess heating over the plateau area (Fig. 6a). When the height of the plateau is increased to half of the modern plateau, we see that the peak of diabatic heating shifts poleward. The contour lines over India, which represents heating concentrations, begins to spread and converge above the Half-Plateau. The same transition can be said when we employ the Himalayan-Wall configuration (Fig. 6b and 6c). However, as the Tibetan Plateau reaches its full elevation, excess diabatic heating over the plateau can be observed (Fig. 4b) and we may draw

similarly conclusions when the plateau height is doubled (Fig. 4d). The overall heating response of the Asian continent due to the rise of the Tibetan Plateau becomes dramatically higher when the plateau reaches a certain elevation. Thus, as the plateau progressively increases in elevation diabatic heating becomes more significant when trying to understand planetary sea-land thermal gradients that occur over southern Asia (Wu et al., 2012; Chen et al., in review).

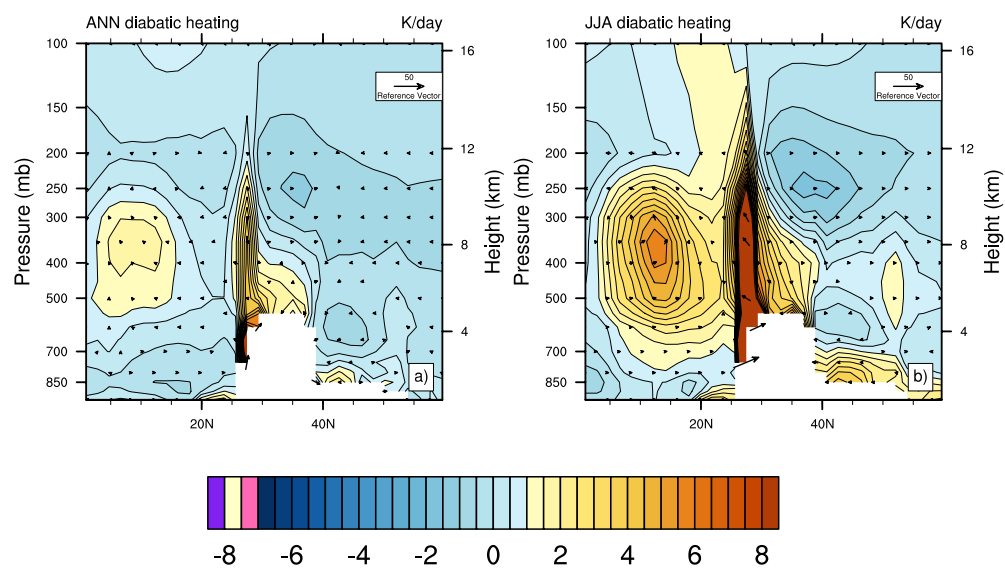


Figure 4: Meridional transect from 0° to 50°N with mean zonal diabatic Heating ( $\text{K day}^{-1}$ ) over longitudinal bands 80° to 90°. Vectors are omega ( $\text{Pa day}^{-1}$ ) and have been scaled by  $10^4$  to highlight vertical velocity.

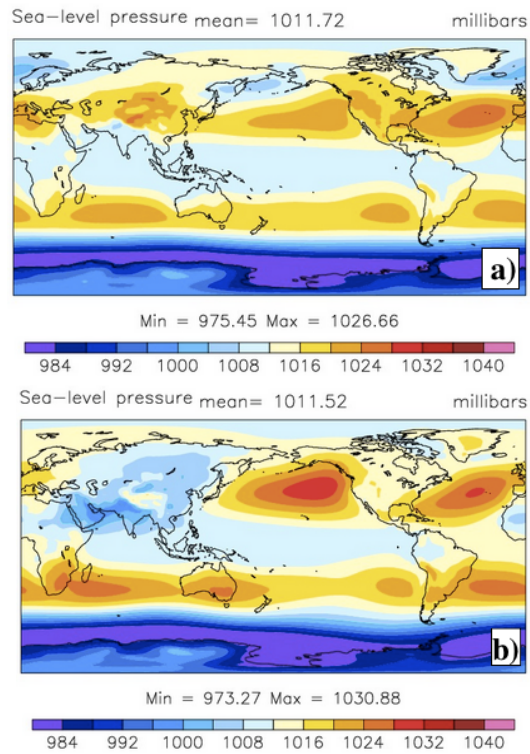


Figure 5: Regular-Plateau simulation, illustrating annual mean sea-level pressures (a) and boreal summer means (b) in milibars.

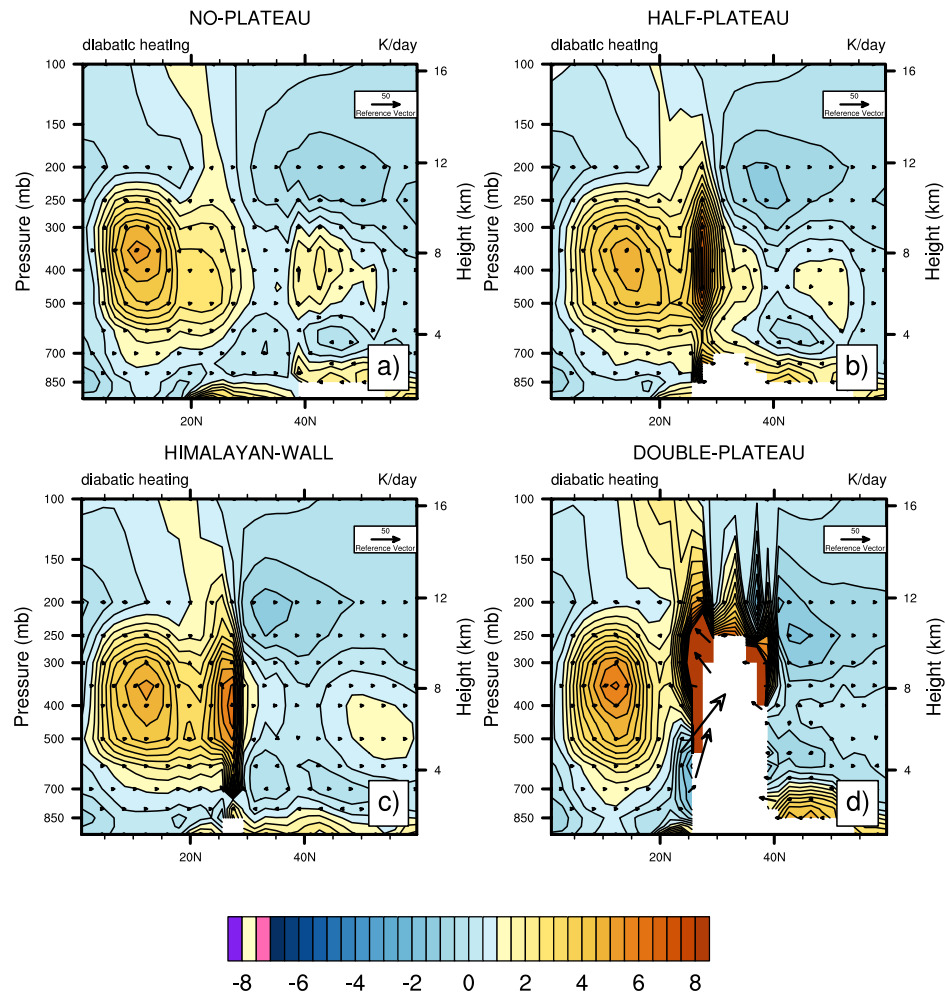


Figure 6: The descriptions for this plot are the same as figure caption 4, instead we have modern CAM4 simulations: No-Plateau (a), Half-Plateau (b), Himalayan-Wall (c) and Double-Plateau (d).

#### 4.2.2 Divergence and Precipitation Over Asia

Trenberth et al. (2000) associated seasonal wind reversal over respective regions as a function of large-scale overturning in the atmosphere. They concluded that such persistent overturning was due to seasonal migration of peak insolation across the equator. As solar radiation heats the surfaces, the surrounding air mass becomes heated which induces convection and forms a low-pressure system. In this section we analyzed

the divergence of wind that corresponds with high and low surface pressures systems over the Asian continent. Usually when considering stationary eddies or convective systems, increased upper-level wind divergence is associated with lower surface pressures and/or an increase in atmospheric heating.

For our simulations, we computed the divergence of wind at the 200 mb vertical level. Figure 7 and 8 shows positive numbers as divergence while negative numbers correspond to convergence, and vectors represent horizontal wind strength and direction. In addition, anomalies were computed to show differences between simulations. Looking at our JJA in our control simulations, we can see that a strong divergence feature resides on the slopes of the Himalayan Mountains, the Arabian Sea, Bay of Bengal and over Southern Asia. In general, the divergent winds at 200 mb are centered over 20°N, and strong convergence is found near 35°N west of Tibetan Plateau.

As we perturb the atmosphere by adding and removing the Tibetan Plateau, we can see in figure 8 (a, b, e, and f) that overall distribution of divergence and convergence of wind during JJA months are similar. We observe a linear increase in divergence over the Himalayan Mountains as the Tibetan Plateau increase in elevation. In addition, looking at our Himalayan-Wall configuration, a persistent decrease in divergence is observed over the slopes of the Himalayan Mountains and has a stronger convergence west of the Himalayan Mountains (Fig. 8g). However, as we double the height of the plateau, we see a stronger convergence behind the Tibetan Plateau (Fig. 8f and 8g). We can see from anomaly plot (Fig. 8c), that as we remove the plateau we have a reduction

of divergence over the slopes of the Himalayan and Tibetan Mountain ranges, however positive anomaly is seen behind the plateau and over Bangladesh.

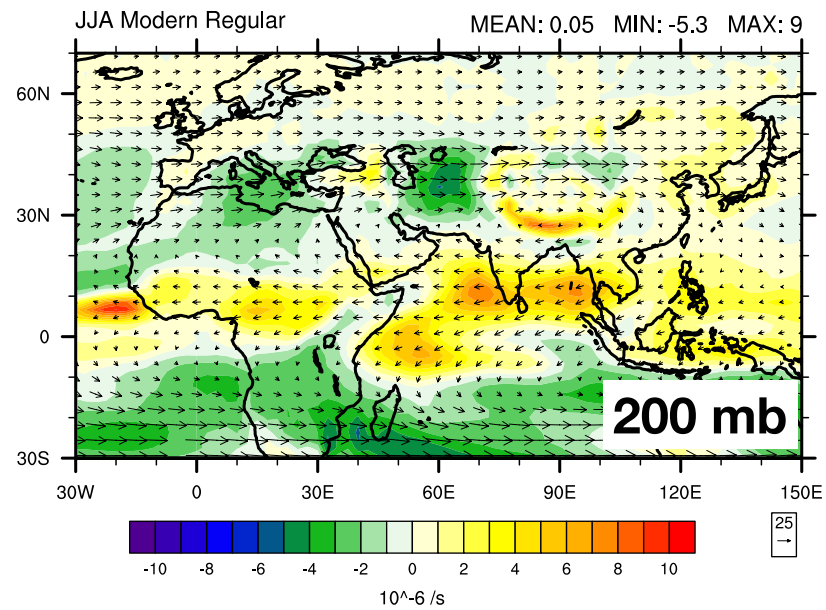


Figure 7: JJA summer months divergence of wind at 200 mb pressure level. Divergence is scaled by multiplying units by  $10^6 \text{ (s}^{-1}\text{)}$  and vector magnitudes were plotted to show direction of wind.

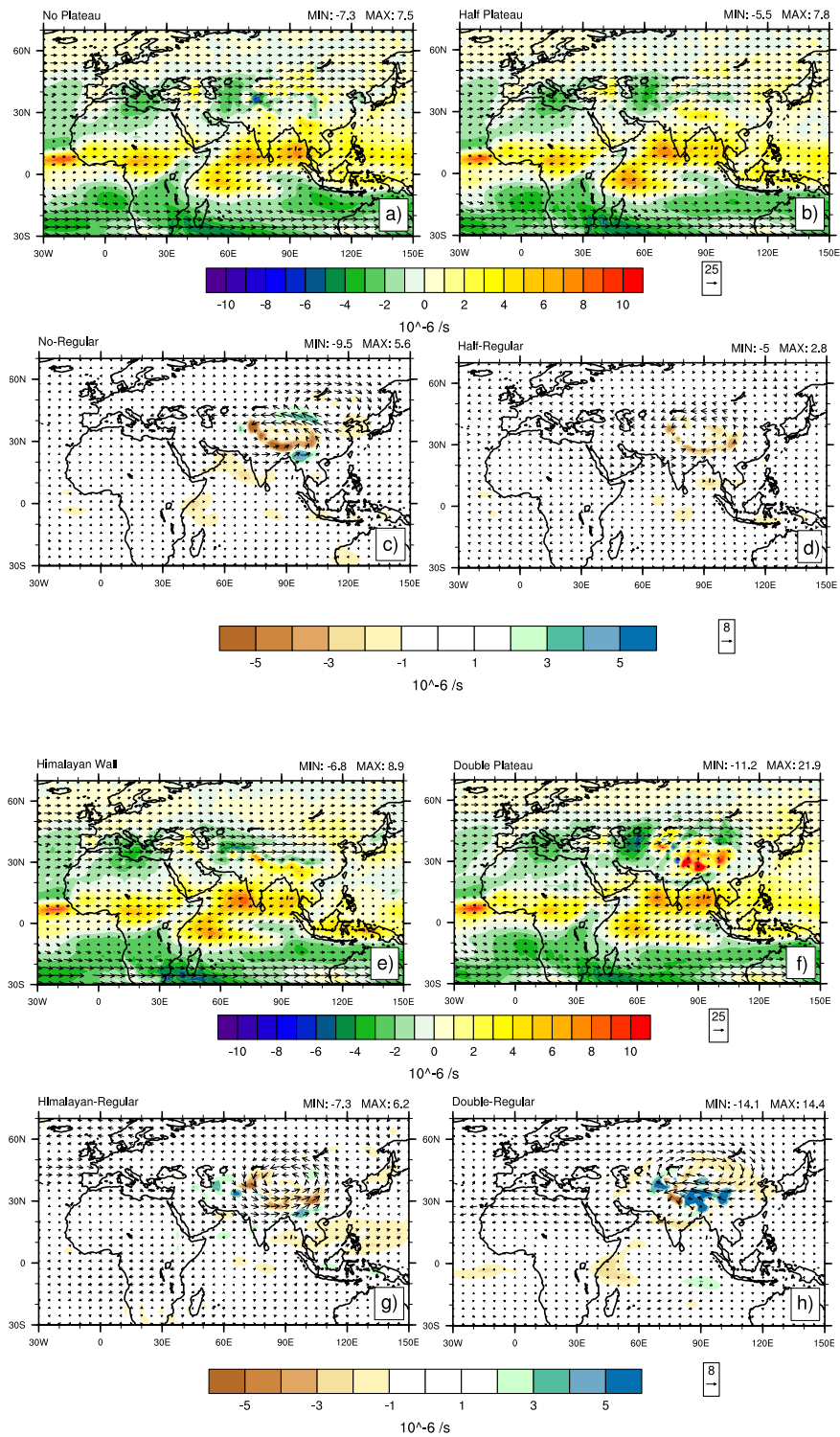


Figure 8: The description for this plot is the same for figure caption 7. Plots a, b, e and f represents our perturbed simulations while plots c, d, g, and h are anomaly plots (test-control).

When looking at the overall JJA precipitation distribution around Asia (Fig. 2a), we see that the majority of rainfall lies near and north of the equator, and crosses over Southern Asia, well into Central Asia (Fig. 9a). The migration of this precipitation band has been hypothesized as part of the seasonal migration of solar insolation, and is highly influenced by orography (Trenberth et al., 2000, Wang, 2006; Zhang and Wang, 2008). Figure 9 contains boreal summer precipitation rates centered over Asia. It has our four perturbed simulations (9 a-d), including our anomaly plots (9 e-h) to illustrate the impact of the plateau on precipitation rates over Asia.

In our No-Plateau simulation, we observe larger rainfall occurring in India and Bangladesh with precipitation max of  $18 \text{ mm day}^{-1}$  (Fig. 9a). When looking at our anomaly plots we see that not only does the precipitation rate increase, its extent also increases as well. The precipitation extent reaches well behind the Tibetan Plateau at  $45^{\circ}\text{N}$ ; no other simulations exhibit this behavior. In contrast, precipitation rates over around the Tibetan Plateau and the coastline areas of India's subcontinent decrease drastically with an anomaly minimum of  $-22 \text{ mm day}^{-1}$  (Fig. 9a and 9e). This reduction of precipitation over the Tibetan Plateau is seen throughout simulations No-Plateau, Half-Plateau, and Himalayan Wall. As we increase the plateau's height to half, the same increase in rainfall can be seen over India while there is some decrease over the eastern side of Asia. When we employ the Himalayan-Wall simulation we can see that the Indo-Asian subcontinent, Arabian Peninsula, Arabian Sea and Indonesia all experience increased precipitation rate, with the anomaly plots showing a maximum change in precipitation of  $6 \text{ mm day}^{-1}$ . Yet



a decrease in precipitation rates can be seen over large regions behind the Himalayan-Wall, in Eastern China and the Philippine Seas, with an anomaly minimum of  $-23 \text{ mmday}^{-1}$  (Fig. 9c and 9g). Doubling the height of the plateau drastically changes the precipitation band over Asia. In our simulation, we show that precipitation rates over the Tibetan Plateau are increased well above our specified range with a maximum of  $152 \text{ mmday}^{-1}$ . While the more southern regions of Indo-Asia, East Asia and the Arabian Sea all experience a decrease in precipitation rate with anomaly minimum rates of  $\sim 8 \text{ mmday}^{-1}$  (Fig. 9d and 9h).

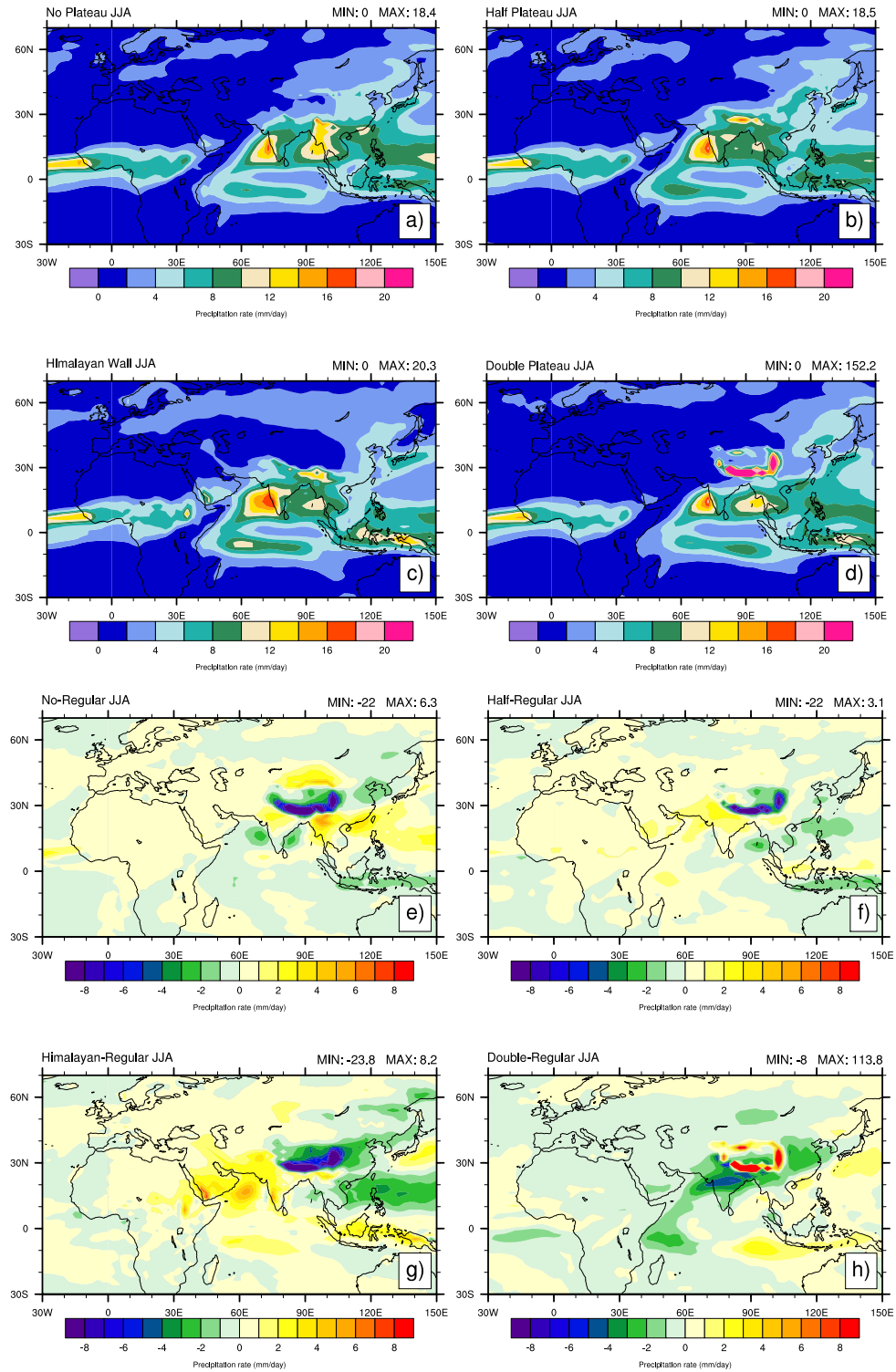


Figure 9: Precipitation rates of our four sensitivity test cases are plotted (a-d) and precipitation anomaly plots are plotted (e-f) as test-control.

### 4.2.3 Mean and Transient Integrated Moisture Transport

To measure large-scale flows in our simulations, we took the time-mean interval of moisture flux and removed small scale eddies represented in our model by  $\overline{U} \overline{Q}$ . By doing this, we can separate slowly varying mean fields such as large-scale stationary eddies and rapidly evolving turbulent flows such as transient eddies  $\overline{U'} \overline{Q'}$ . This methodology is known as Reynolds Averaging (Holton, 2012) and was mentioned prior in section 2.3 (Mintz, 1974). Moisture transport in the mid-latitude is dominated by transient eddies that forms due to baroclonic instability. We should also keep in mind that baroclinic wave activity is strongest during wintertime when the temperature gradient between the poles and the equator are the strongest. In this section we calculated both mean and transient moisture transport at a given integrated pressure level to provide the origin of moisture observed in our simulation (Fig. 10-13). In general, we can see between figure 10 and 12 that the mean moisture is an order of magnitude higher than the transient transport.

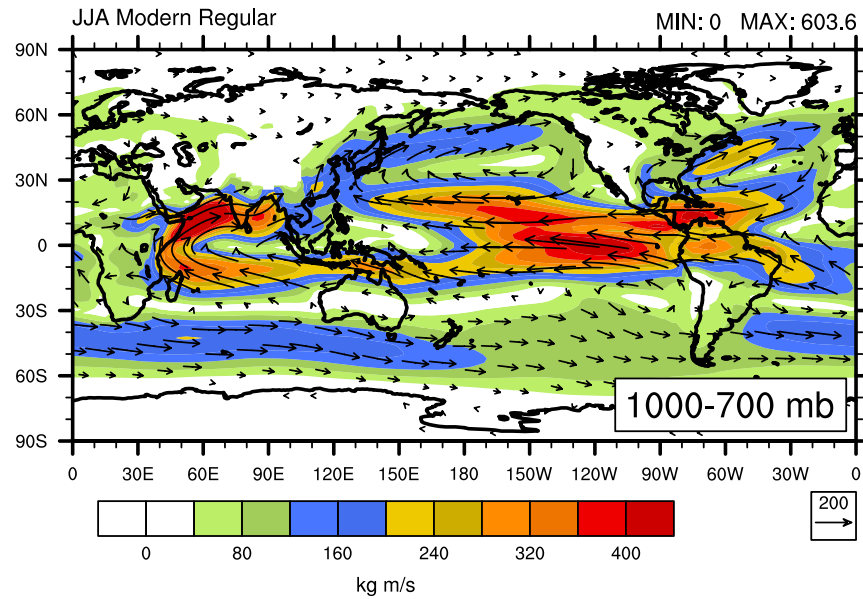


Figure 10: Global mean integrated moisture flux from 1000 to 700 mb pressure levels during boreal summer. Vectors represent wind magnitudes and directions.

When looking at the NH summer, mean transport at pressure levels 1000-700 mb in our control case, we see that moisture transport is concentrated at the equator and more so at central Pacific, and moisture over the Indian Ocean are transported poleward (Fig. 11). We can see that removal of the Tibetan Plateau lowers mean moisture transport where the SAM and EAM reside. In addition, we can see that JJA mean moisture transport are much stronger in the oceans and gets weaker over land. We see similar results when looking at the Half-Plateau simulation. However looking at our Himalayan-Wall simulation we see that mean moisture transport is substantially reduced in several regions, including Southern Asia, Eastern Asia and South America. Finally, the opposite is seen when considering our Double-Plateau case. Its presence

induces stronger mean moisture transport over Asia and the central Pacific compared to our other simulations.

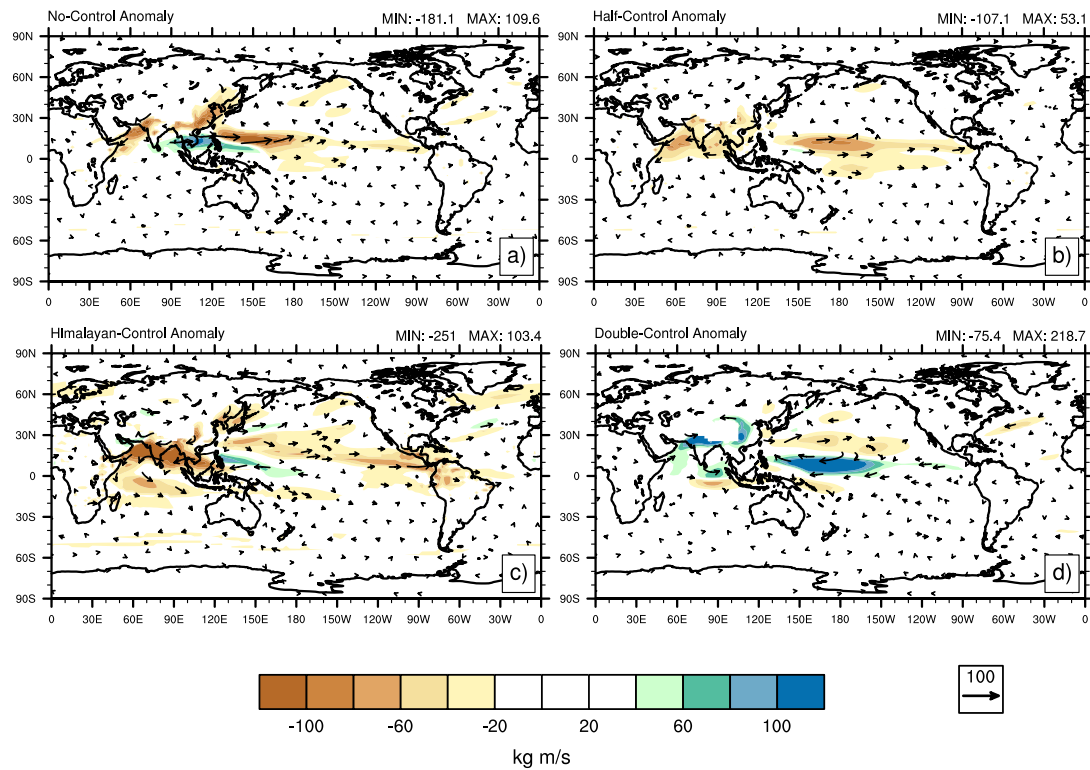


Figure 11: The same description for figure caption 11 is used for this figure, with plots a-d as our anomaly plots.

Fast turbulent moisture transports are mainly seen in mid-latitude regions (Fig. 12 and 13). During the NH summer, transient eddy transport resides on the eastern flanks of large-scale mountain belts (Fig 12). Our anomaly plots (Fig 13 a-d) shows the Tibetan Plateau minimally influencing global transient eddies, where its main effects only exist on the Asian continent. When we remove the plateau, we see an increase in transient moisture flux at the Bay of Bengal and a decrease at the western section of Asia (Fig 13 a-c). Most notable in our anomaly plot is the Himalayan-Wall simulation,

where transient eddies over Central Asia as well as northern section of Arabia increase dramatically. Such increases in transient eddies are counter balanced by weakening over southwestern and northeastern regions of Asia. Our Half-Plateau simulation and Double-Plateau simulation shows minor changes in transient eddy transport.

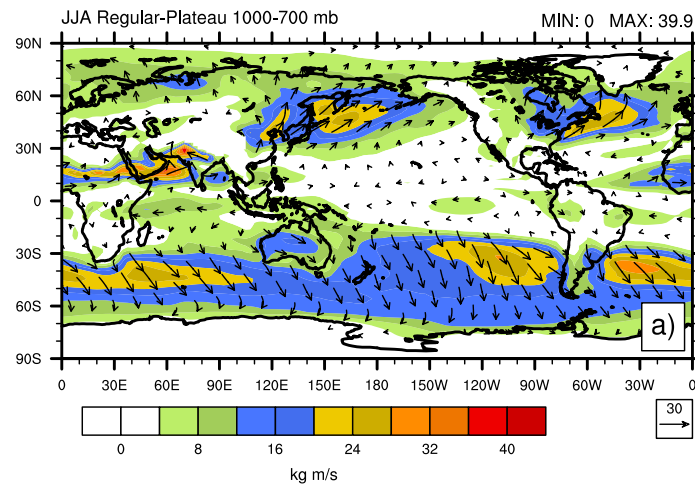


Figure 12: Global transient integrated moisture flux from 1000 to 700 mb pressure levels of JJA summer months is plotted on a color contour map with vector magnitudes plotted to show wind direction.

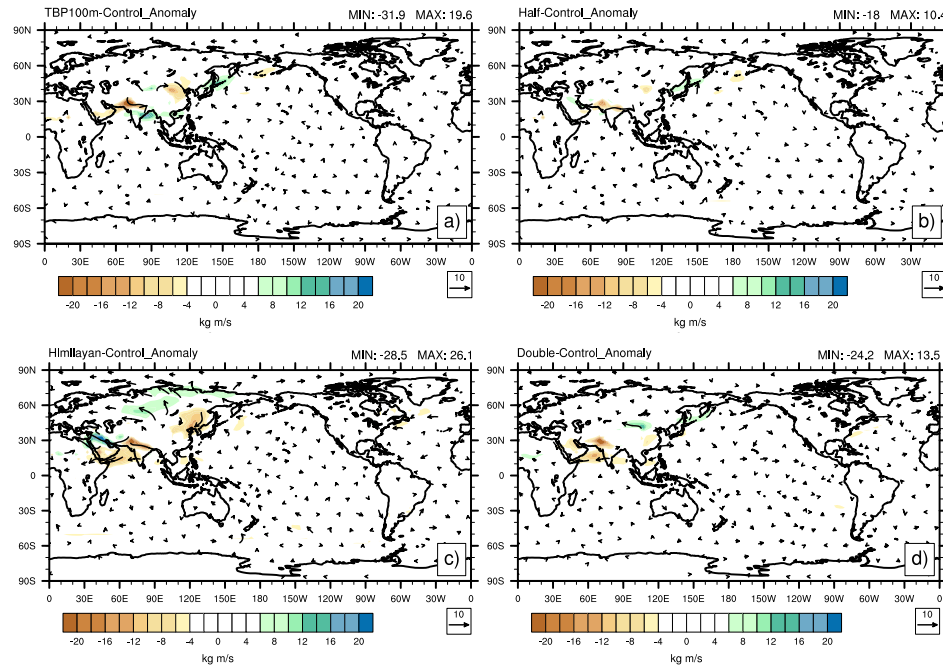


Figure 13: The same description for figure caption 13 is used for this figure, with plots a-d as our anomaly plots.

#### 4.3 Global Precipitation Distributions and the Global Monsoon Index

In this section we consider the impact of the Tibetan Plateau on the global precipitation and how it influences the dimensions of the global monsoon. We can see that during NH summer, the ITCZ's migration strongly preferences Asia and as mentioned before in section 4.2.2, the precipitation rates over Southern Asia are substantially increased compared to other locations at the same latitude (Fig. 14b). During SH summer months, the ITCZ strongly influences precipitation rates over Australia, South America, and South Africa (Fig. 14c). In addition, we can see large swaths of precipitation in mid latitudes bands over the North Pacific in DJF and the

South Pacific in JJA months, which are a function of turbulent moisture transport, which were presented in earlier section 4.2.3.

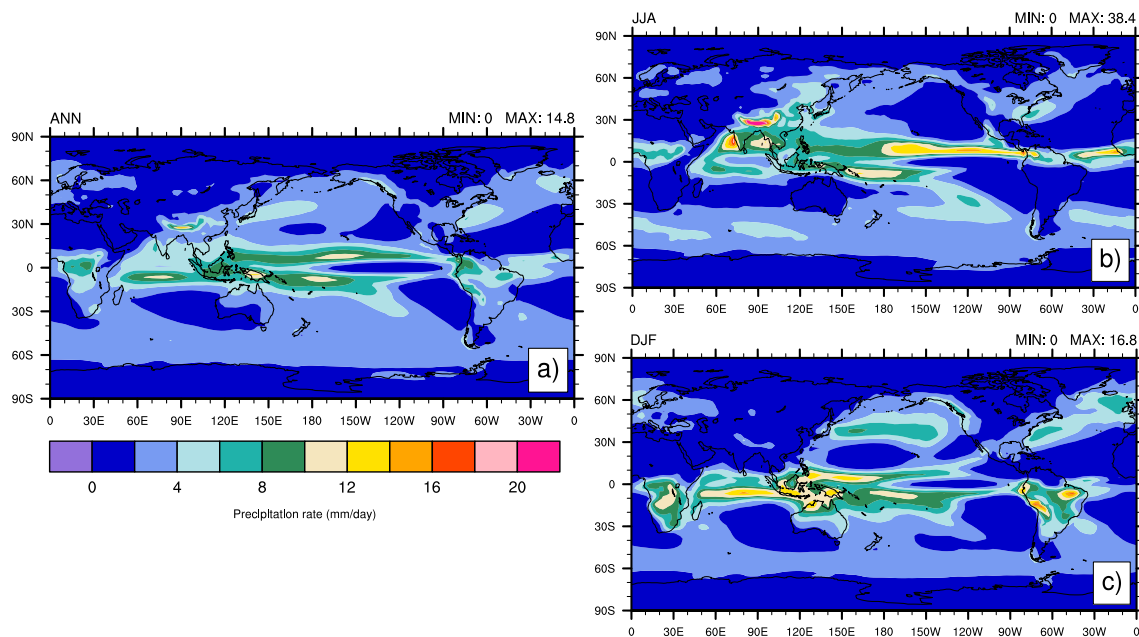


Figure 14: Global precipitation rates of control case with annual (a), JJA months (b) and DJF months plotted.

To identify the effects of the Tibetan Plateau on global precipitation, we present eight anomaly plots representing the differences between each of our test simulations compared to our standard CESM simulation (Regular-Plateau) (Fig. 15 a-f). We show in our anomaly plots that during JJA months (Fig. 15 a-d) the main areas impacted by the Tibetan Plateau are the immediate surrounding area. Furthermore, as pointed out in section 4.2.2, increased precipitation rates over the Indian subcontinent and decreased precipitation rates over Tibet are simulated with a lower the plateau. Also, there is an overall decrease in precipitation in non-elevated areas when plateau elevation is doubled and a strong bimodal precipitation distribution in the Himalayan-Wall



simulation. Looking at DJF anomalies (Fig. 15 e-h), we see that in our No-Plateau simulation the Indian Ocean experiences significant increase in precipitation, and drying over the Pacific islands (Fig. 15e). Additionally, our Double-Plateau run shows similar drying areas as our No-Plateau simulation, but exhibits strong positive orographic precipitation (Fig. 15h). The Himalayan Wall simulation shows a weaker ITCZ band above Papua New Guinea, correlated with positive precipitation north of the equator (Fig 15g).

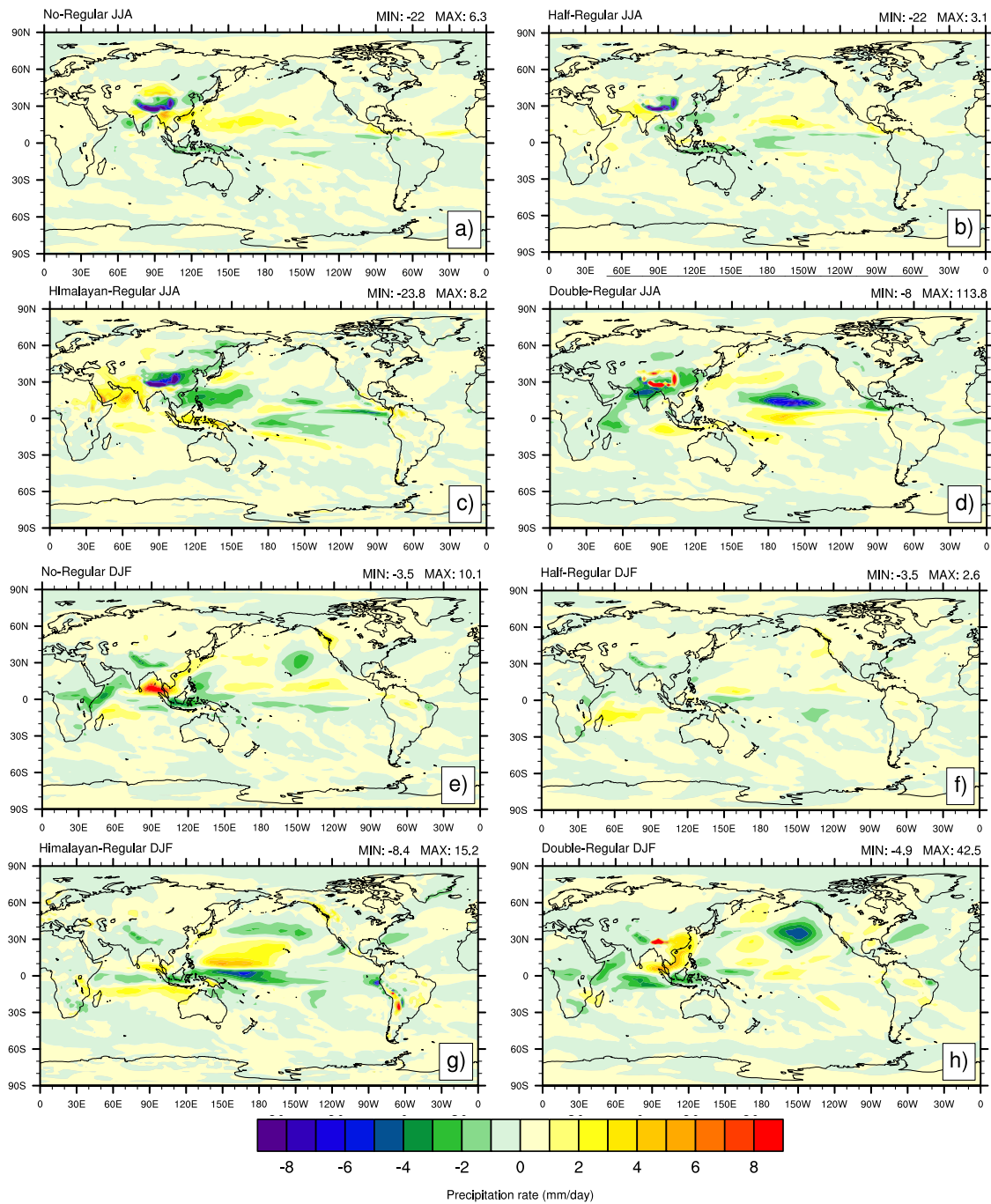


Figure 15: Anomaly plots of global precipitation rates with JJA months as plots a-d and DJF months as plots e-h.

In this section we applied the global monsoon metric from Zhang and Wang (2008), to highlight areas that have precipitation rates above  $3 \text{ mm day}^{-1}$  and are

extremely seasonal (Fig. 16 and 17). Similarly to Zhang and Wang (2008), we chose 55% as our criterion for precipitation seasonality (See section 3.2). In our Regular-Plateau simulation, we observe main monsoonal regions are as follows: Asia, West Africa and North American for extended NH summer months (MJJAS), and South Africa, Australia and South America for extended SH summer months (NDJFM) (Fig. 16). It is important to reiterate, that this monsoon index positive numbers do not correlate with higher precipitation rates but a higher percentage of summer precipitation compared to the annual.

Using this method, we show that the global monsoon sensitivity to elevation change of the Tibetan Plateau are mainly concentrated over Asia, and are substantially affected in their dimensions and seasonality (Fig. 17). In addition, other monsoon regions generally retain the same spatial distribution, however, individual monsoon seasonality slightly varies (Fig. 17). More specifically, we can see in our No-Plateau simulation that the SAM dominates both the southern and eastern regions of Asia and its seasonality over the Indian subcontinent becomes greater (Fig. 17a). In addition, Eastern China, north of the Philippines and across the Central Pacific Ocean in our No-Plateau simulation exhibits increased seasonality and precipitation rates above  $3 \text{ mm day}^{-1}$  (Fig. 17a). As we increase the plateau's elevation to Half-Plateau, the EAM and SAM have the same features as our control case (Fig 17b). When employ the Himalayan-Wall, we see that the SAM becomes more seasonal, however, the EAM decreases in seasonality and dimensions (Fig 17c). The most significant change observed through out all our runs is seen in our Double-Plateau simulation. It shows a decreased summer

monsoon features over East-central Asia, and a smaller monsoon band over East China Sea. Although a distinguishable division between the SAM and EAM is seen, their seasonality is similar to that of our control case.

Generally we see that the NH monsoon regions are slightly influenced by the elevation of the Tibetan Plateau. The opposite is seen over the SH, where SH Monsoon systems do no change regardless of the Tibetan Plateau's height. Additionally, we see that seasonality over these systems slightly varies when you alter the plateau's elevation, however, there are no consistent seasonality pattern observed throughout our simulations. Lastly, changing the Tibetan Plateau's elevation only impact the AM.

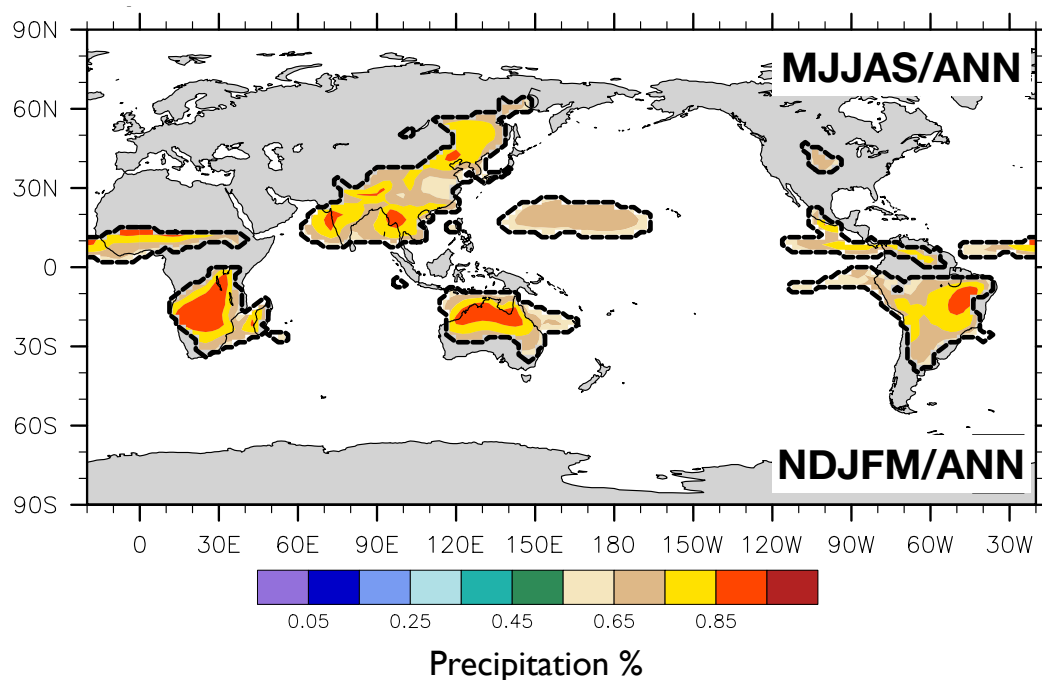


Figure 16: Regular-Plateau simulation showing extended seasonal cumulative precipitation rates ( $\text{mm day}^{-1}$ ) normalized and divided by annual cumulative precipitation rates ( $\text{mm day}^{-1}$ ) to show percentage of precipitation occurring seasonally. Areas highlighted are regimes with precipitation rates above  $3 \text{ mm day}^{-1}$ . Extended months are MJJAS for NH months (plotted from  $0^{\circ}$ - $90^{\circ}\text{N}$ ) and NDJFM for SH months (plotted from  $0^{\circ}$ - $90^{\circ}\text{S}$ ). Individual square boxes highlight each monsoon areas.

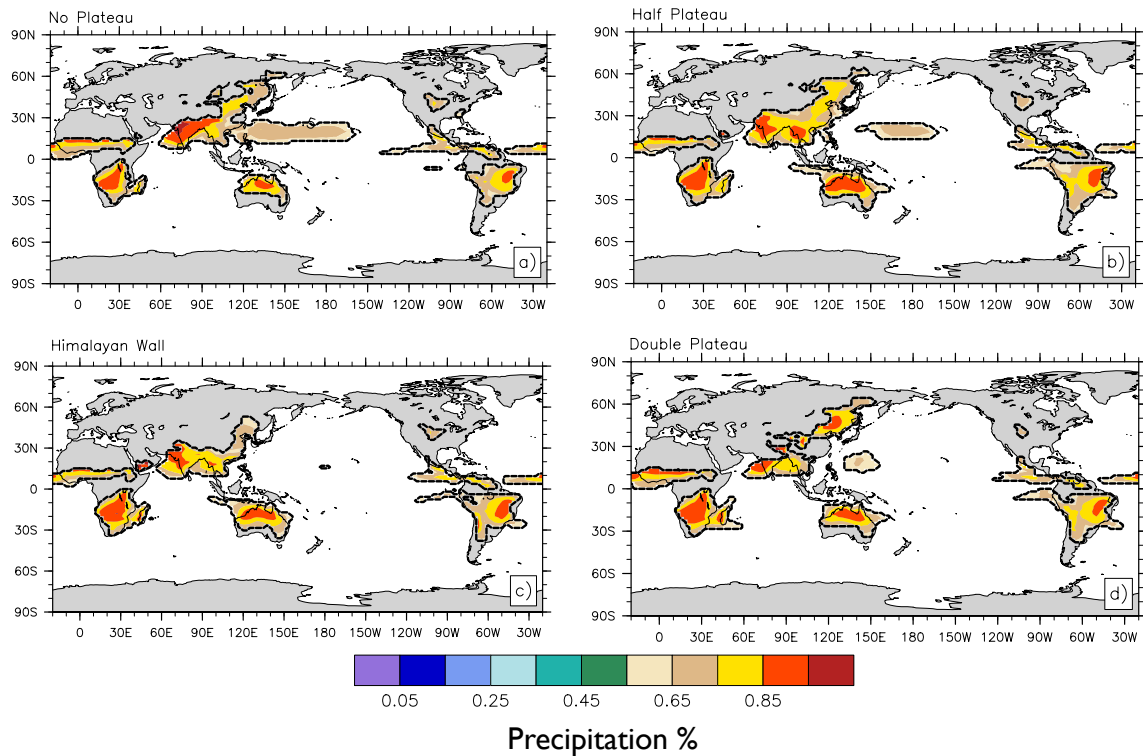


Figure 17: This figure has the same description for figure caption 16. Highlighting our sensitivity cases No-Plateau (a), Half-Plateau (b), Himalayan-Wall (c) and Double-Plateau (d).

#### 4.4 Preliminary CAM 5 comparisons

The comparison between pre-industrial CAM4, and CAM5 simulations shows minor differences in global JJA mean surface temperature, while JJA mean surface latent heat flux in CAM5 simulations is  $\sim 10 \text{ W m}^{-2}$  greater in mid latitude regions than CAM4. In addition, annual percent total cloud cover is much greater in CAM5, while annual planetary boundary layer height are much lower by  $\sim 10\%$  ( $\sim 60 \text{ m}$ ) (not shown in figures). These wide differences in surface temperature, and heating, boundary layer height distribution surprisingly do not impose large changes on global precipitation rates.

Although precipitation bands during summer months (JJA NH, and DJF SH) are drastically different between CAM4 and CAM5, our monsoon index do not suggest that these changes precipitation are necessary analogous to changes in monsoon distribution (figure not shown). However, these changes do show some promise when identifying spatial distribution of precipitation over Asia. We can see that CAM5 resolves the lack of rain band on the southern regions of North America and eastern parts of Asia during JJA months. Nonetheless CAM5 versus CAM4 simulation show do hold potential for future work on the global monsoon.

When we analyzed how global precipitation change when you increase or decrease the elevation of the Tibetan Plateau in preindustrial boundary conditions and CAM5 GCM. The removal of the plateau during NH summers (No\_TBP\_CAM5) shows weakening of orographic precipitation ( $\sim 10 \text{ mm day}^{-1}$  less) but adding moisture behind the plateau ( $\sim 2\text{-}4 \text{ mm day}^{-1}$  more). Also, the Arabian Sea and Arabian Peninsula have  $\sim 2\text{-}3 \text{ mm day}^{-1}$  more precipitation than the regular plateau height. Double the plateau height has the opposite effect: it decreases precipitation rate over southwestern and southeastern portion of Asia, while increases precipitation rates at the slopes of the plateau (Fig. 18a and 18b). We also see large changes in precipitation rates over the Pacific Ocean and over the Pacific Islands. While looking at SH summer (Fig. 18c and 18d), major changes in precipitation rates are seen above the equator when you remove the plateau and the opposite when you double the plateau's elevation. The overall effects of adding or removing the Tibetan Plateau on our Pre-industrial CAM5

simulations are comparable to our Modern CAM4 simulations, which suggest that our simulations are robust in nature within two significantly different atmospheric modeling framework.

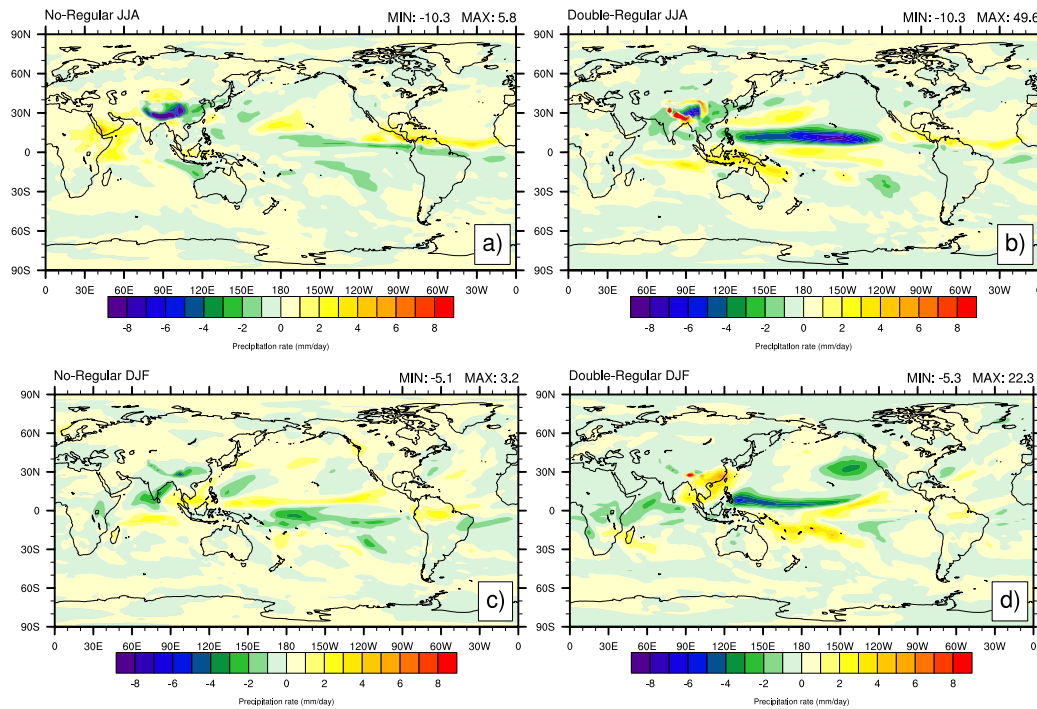


Figure 18: Anomaly plots of CAM 5 No-Plateau and Double-Plateau simulations for global precipitation rates are plotted for JJA months (a-b) and DJF months (c-d.)



## 5. DISCUSSION

The comparisons between our cases show common features. Reduction of Tibetan Plateau elevation results in increasing JJA mean precipitation rates over Southern Asia and a decrease in orographic precipitation, and vice versa when you increase the height of the plateau. To understand the increased precipitation pattern seen over Southern Asia we need to consider the following: diabatic heating over the subcontinent, allocation of heat over the Tibetan Plateau, and meridional moisture convergence by the mean stationary flow and transient eddies. In this section, we discuss the value of the plateau and whether or not its ability to produce significant diabatic heating is a mechanism that truly impacts the Asian monsoon.

### 5.1 Precipitation regimes over Southern Asia

We saw in Section 4 that the elevation of the Tibetan Plateau and the Himalayas has significant importance when considering the distribution of the Asian monsoon. However, in the absence of a plateau, the SAM is broader and extends further inland (Fig 17). In addition, even a plateau that is only half of modern or even a Himalayan-Wall creates a modern like SAM pattern, with the exception of our Double-Plateau simulation. This suggests that the SAM exist regardless of the plateau's elevation (Huber and Goldner, 2011; Wu et al., 2012). In addition, precipitation regimes over Southern Asia

and orographic precipitation in our simulations are consistent with Chen et al. (in review). They showed that the precipitation rates over the southwest region of Asia are increased when topography is lowered. This observation is relatively new and disagrees with other simulation results by Hahn and Manabe (1975), Kutzbach et al. (1989 and 1993), and Kitoh, (2002 and 2004). Furthermore, the largest area impacted by the rise of the plateau is Eastern Asian and regions behind the plateau. We showed that the strengthening of EAM strengthens when the height of the Tibetan Plateau is increased (Kitoh, 2002), however, double the height of the plateau provides a clear division between the SAM and EAM.

Although we see moisture flux in Asia decreases when we remove the Tibetan Plateau and the Himalayan mountains, we also see an increase in precipitation rate over the lower subcontinent. This conflict in hydrological cycle can be explained by analyzing the distribution of divergence at 200 mb (Fig. 7 and 8). As seen in our control simulation, divergence over Asia is allocated in both the Asian subcontinent and over elevated topography (Fig. 7). However, when we remove the Tibetan Plateau, divergence over the plateau decreases (Fig. 8c and 8g) and this loss in divergence over the plateau is interconnected to the loss of excess diabatic heating created by the plateau (Fig. 4b) (Prell et al., 1993; Trenberth et al., 2000). However, removing the plateau allows divergence to be concentrated behind the Tibetan Plateau and over Bangladesh, which is accompanied by increase in precipitation rates over these regions. This redistribution divergence is further exacerbated, when we remove the Tibetan Plateau but keep the Himalayan Wall. We see the same redistribution of high altitude divergence, yet in

comparison to our No-Plateau simulation, it is unclear why we see such a drastic increase in precipitation rate when we invoke the Himalayan-Wall configuration. For this study, we did not investigate whether or not in our simulations prevented extratropical air from entering Southern Asia (Boos and Kuang, 2010), however, we do observe the same decrease in divergence over the plateau.

When looking at our Double-Plateau simulation, we see that diabatic heating is strongly concentrated over the Tibetan Plateau. However, in this case we see weaker precipitation rates over the subcontinent (Fig. 9h), a stronger orographic precipitation (Fig. 9h), and an increase in mean integrated moisture transport (Fig 12d). We suggest that moisture transport and orographic precipitation increases linearly, while precipitation rates over Southern Asia decreases linearly as you increase the height of the plateau. These results supports Wu et al. (2012), where they saw we see concentrated precipitation at the slopes of the plateau, and the large flux of moisture. In addition, we support the conclusions of Huber and Goldner (2011), Wu et al. (2012) and Chen et al. (in review), such that large moisture transport from the equator toward the pole is correlated to the excess diabatic heating that is seen at the front of the plateau (Fig. 6d). In support, we show that the tremendous heating produced by our double topography acts as a moisture attractor via increased convection, invoking preferential deposition of precipitation at the slopes of the mountains. Our results suggest that without the plateau this moisture conveyor belt over Southern Asia is most likely weaker.

## 5.2 The Global Monsoon

Throughout the suite of simulations we produced, we found that much of the monsoonal regions remained unchanged, regardless of the height of the topography. Similarly to studies done by Huber and Goldner (2011), where they determined that in a warmer climate such as the Eocene, the global monsoon's occurrence was largely unaffected by the height of the Tibetan Plateau. Furthermore, they hypothesized that thermal gradients produced in a warmer climate system could be damped, such that in a colder time period these planetary sea-land breeze may have a larger affect on the global monsoon. Our study showed that even in modern settings and varying the height of the plateau, the global monsoon with the exception of the SAM and EAM, is largely unaffected. We saw that the largest anomalies produced by orographic perturbation were located near the plateau and across the Central Pacific Ocean.

It was interesting that the global moisture transport via transient eddies with the exception of Asia were unaffected by the plateau's elevation (Fig. 13). Yet when looking at global mean moisture flux, the Asian continent areas near the equator were substantially changed (Fig. 11). In addition, we determined that global precipitation distribution is largely unaffected by Tibetan Plateau's elevation, with the exception of the Asian continent and large portion of the Pacific Ocean.

The general circulation seen in our Half-Plateau simulation suggests that there is a Goldilocks height where atmospheric flow becomes significantly altered (Kutzbach et al., 1989; Molnar and England, 1993) (Fig. 15b and 15f). Furthermore, looking at our Himalayan-Wall topography we see that the horizontal width of the plateau is also

another physical property that has a large affect on global circulation. The combination of both physical mechanisms shows significant redistribution of moisture in the Pacific. This is due to dramatic decrease in zonal wind at the latitude bands where Tibetan Plateau is found (not shown) and an increase in adjacent latitude bands. Furthermore, we can see that keeping the Himalayan Mountains elevated and removing the Tibetan Plateau has similar negative effects on zonal wind transport, but its impact is much closer to the Asian continent and does not span across the length of the Pacific Ocean.

Generally, our findings are consistent with earlier topography studies by Ruddiman et al. (1989), Abe et al. (2004), Huber and Goldner (2011). We saw that annual surface temperature over land and annual sea surface temperature linearly increase as the Tibetan Plateau's height decreases (Fig. 19). Intriguingly, we see an increase in annual precipitation over land when you increase the plateau's height, except when we double the plateau's elevation (Table 2). We confirm that impact of Tibetan Plateau elevation change on NH circulation is minimal and generally insignificant in the SH. For further diagnostics of our results see Table 2.

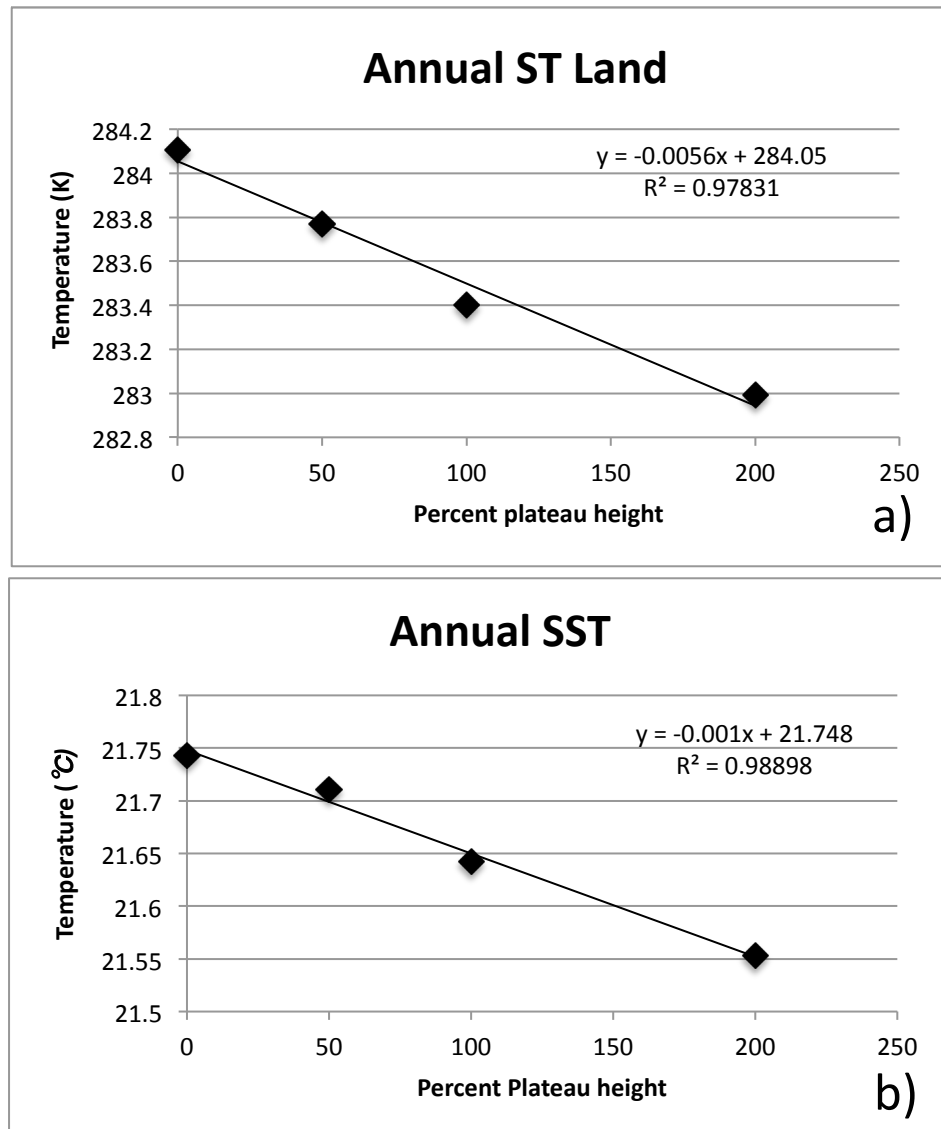


Figure 19: Annual surface temperature (a) and annual sea surface temperature (b) are plotted against percent plateau height with 0% as No-Plateau, 50% as Half-Plateau, 100% as Regular-Plateau and 200% as Double-Plateau. A fitted linear regression with and  $R^2$  of 0.978 for ST Land and 0.988 for SST was taken to present how surface temperature responds to large orographic perturbation.

Table 2: Diagnostics variables taken from all modern simulations

	REG-Plateau	NO-Plateau	HALF-Plateau	DOUBLE-Plateau	HIMALAYAN
RESTOM	.219	0.218	0.174	0.086	0.188
RESSURF	.220	.0206	0.173	0.084	0.187
PRECT LND	2.369	2.337	2.386	2.330	2.466
PRECT OCN	3.333	3.365	3.353	3.303	3.323
PREH2O	28.304	28.704	28.594	28.079	28.743
QFLUX	2.956	2.969	2.975	2.923	2.983
SST	21.642	21.743	21.711	21.553	21.718
TS	289.662	289.916	289.837	289.468	290.054
TS LAND	283.401	284.107	283.771	282.994	284.395
LWCF	29.456	29.482	29.451	29.382	29.563
SWCF	-52.575	-52.302	-52.586	-52.275	-52.612

### 5.3 CAM5 Comparison

Even with the addition of the new aerosol physics and cloud parameterization scheme in CAM5, and a switch to pre-industrial boundary conditions, it is remarkable how similar CAM5 and CAM4 responded to orographic perturbation. Furthermore, although we see the same biases when comparing spatial patterns to other observational data products (not shown), such as the formation of the split ITCZ, we showed that our simulations response to orographic perturbation were consistent with each other. However, we do see changes in precipitation rates, but overall the spatial patterns are similar. For example precipitation bands over the plateau were still concentrated at the slopes of the mountains, while removing the plateau still increased precipitation behind the plateau. Doubling the plateau, we saw overall decrease in precipitation in the lower subcontinents of Asia and while simultaneously increasing precipitation rates over its slopes. Furthermore, extreme changes are seen over the Pacific Ocean. Doubling the topography induced a massive decrease of precipitation

near the equator. In addition, precipitation response in our No-Plateau simulations shows the same increase in precipitation over the Arabian Sea and India as our CAM4 modern No-Plateau and Himalayan-Wall simulations.



## 6. CONCLUSION, FUTURE DIRECTIONS AND IMPLICATIONS

We studied the effects of altering the plateau height on the Asian and the global monsoon system using the NCAR CESM1 in slab ocean configuration with modern boundary conditions. We illustrated that doubling the plateau height decreases the strength of the Asian monsoons over all of India and most of central and eastern China, while removing the plateau further extends the reach of the SAM inland, consistent with previous work (Kitoh, 2003; Abe et al., 2004; Chakraborty et al., 2006; and Molnar et al., 2012). In addition, lowered topography simulations such as No-Plateau, Half-Plateau and Himalayan-Wall shows stronger precipitation bands over the lower regions of southern Asia more than the full plateau configuration. This phenomenon was caused by the overall increase in surface temperature, increase in diabatic heating and the redistribution of precipitation when you lower the plateau. Further reevaluation of Boos and Kuang (2010) has shown that the Himalayan-Wall simulation strengthens the SAM. However this simulation cannot fully explain the SAM system's existence because the removal of any elevated regions (No-Plateau) still allow the SAM to persist and also increase its strength, contrary to Boos and Kuang (2010). This suggests a level of model dependence in their results. Thus, this study concludes that the evolution of the SAM is not solely reliant on orography.

One of the most important finding of this paper is the precipitation distribution of our double topography. We showed that an object as high as our Double-Plateau simulation becomes a moisture attractor. Decreasing precipitation in its immediate vicinity while enhancing the production of precipitation over its slopes. Whether or not this is due to increase diabatic heating created by plateau or extensive orographic lifting due to the plateau's height, its ability to preferentially redistribute moisture proves that the existence of the plateau overall effects the hydrologic system and climatology of Asia. In addition, we linear increase in orographic precipitation as you incrementally increase the height of the plateau. Lastly, we have determined in our simulations that the SAM strength over India is much stronger when you lower the plateau's elevation.

Globally, we identified that the implications of changing the plateau height in modern boundary conditions do not substantially change global precipitation rates. As a result, regardless of the plateau height the SAM still existed and overall the global monsoon is unchanged. However, we have shown that the largest impact of the Tibetan Plateau height is seen over the Asian continent and the Arabian Peninsula. Furthermore, we see that circulation over the Pacific Ocean is substantially changed when you either double the plateau or invoke the Himalayan-Wall configuration. This paper supports Kutzbach et al. (1989), Kitoh (1993), Chakraborty et al. (2006) conclusion regarding the induced physical blocking of zonally flowing wind, and rearrangement of pressure systems are induced with an elevated plateau. Nonetheless, our study has shown that in a cooler climate with enhanced temperature gradients, the response of the global

monsoon to Tibetan Plateau's elevation changes is a weak one (Huber and Goldner, 2011).

The comparison between pre-industrial CAM4, and CAM5 simulations has shown global annual mean surface temperature, with CAM5 is substantially warmer than CAM4 (Meehl et al., 2013). The annual global mean surface latent heat flux in CAM5 simulations is also greater than in CAM4. In addition, the annual percent total cloud cover is much greater in CAM5, while the annual planetary boundary layer height is lower than CAM4 (Gent et al., 2011b; Hurrell et al., 2013). These wide variations in surface temperature and heating, quantity of cloud cover, and boundary distribution surprisingly do not impose large changes on the distribution of the summer monsoon systems. Although the precipitation bands during summer months (JJA NH, and DJF SH) are slightly different between CAM4 and CAM5, our monsoon index does not suggest that these changes in precipitation are necessarily analogous to changes in Global Monsoon distribution and precipitation seasonality. Nonetheless, comparison between CAM5 and CAM4 simulations show that Asian Monsoon region and African Monsoon are the only monsoon system that is affected by orography.

Although our CAM5 and CAM4 simulations have similar changes when perturbed by orography and support the robustness of our simulations, further work is necessary to validate the results of our study. Chen et al. (in Review) have shown the importance of ocean circulation to the monsoon and further touch upon the implication of using higher resolution, fully coupled models. In addition, although we suggested that excess diabatic heating over the Tibetan Plateau is an important mechanism, refinement of our

sensitivity studies such as dampening of surface latent heat produced over selected regions (Wu et al., 2012; Boos and Kuang, 2013) in CAM5 configurations is the natural future direction of this study. Lastly, precipitation biases in the model and comparison to other observational data through a more rigorous statistical assessment is a necessary step that needs to be further explored.

## LIST OF REFERENCES

## LIST OF REFERENCES

- Abe, M., Yasunari, T., & Kitoh, A. (2004). Effects of Large-scale Orography on the Coupled Atmosphere-Ocean System in the Tropical Indian and Pacific Oceans in Boreal Summer. *Journal of the Meteorological Society of Japan*, 82(2), 745–759. doi:10.2151/jmsj.2004.745
- Adams, D. K., & Comrie, A. C. (1997). The North American Monsoon. *Bulletin of the American Meteorological Society*, 78(10), 2197–2213. doi:10.1175/1520-0477(1997)078<2197:TNAM>2.0.CO;2
- Anderson, D. M., Baulcomb, C. K., Duvivier, A. K., & Gupta, A. K. (2010). Indian summer monsoon during the last two millennia. *Journal of Quaternary Science*, 25(6), 911–917. doi:10.1002/jqs.1369
- An, Z. (2000). The history and variability of the East Asian paleomonsoon climate. *Quaternary Science Reviews*, Volume 19, Issues 1-5, Pages 171-187
- Bitz, C. M., Shell, K. M., Gent, P. R., Bailey, D. a., Danabasoglu, G., Armour, K. C., ... Kiehl, J. T. (2012). Climate Sensitivity of the Community Climate System Model, Version 4. *Journal of Climate*, 25(9), 3053–3070. doi:10.1175/JCLI-D-11-00290.1
- Boos, W. R., & Kuang, Z. (2010). Dominant control of the South Asian monsoon by orographic insulation versus plateau heating. *Nature*, 463(7278), 218–222. doi:10.1038/nature08707
- Boos, W. R., & Kuang, Z. (2013). Sensitivity of the South Asian monsoon to elevated and non-elevated heating. *Scientific reports*, 3, 1192. doi:10.1038/srep01192
- Bordoni, S., & Schneider, T. (2008). Monsoons as eddy-mediated regime transitions of the tropical overturning circulation. *Nature Geoscience*, 1(8), 515–519. doi:10.1038/ngeo248
- Chakraborty, A., Nanjundiah, R. S., & Srinivansan, J. (2006). Theoretical aspects of the onset of Indian summer monsoon from perturbed orography simulations in a GCM. *Annales Geophysicae*, (2003), 2075–2089.

- Champagnac, J.-D., Molnar, P., Sue, C., & Herman, F. (2012). Tectonics, climate, and mountain topography. *Journal of Geophysical Research*, 117(B2), B02403. doi:10.1029/2011JB008348
- Chao, W. (2000). Multiple quasi equilibria of the ITCZ and the origin of monsoon onset. *Journal of the atmospheric sciences*, 57, 641–651.
- Chen, G.-S., Liu, Z., & Kutzbach, J. E. (n.d.). Reexamining the barrier effect of Tibetan Plateau on the South Asian summer monsoon. *Climate of the Past Discussions*, 9(4), 5019–5036. doi:10.5194/cpd-9-5019-2013
- Danabasoglu, G., & Gent, P. R. (2009). Equilibrium Climate Sensitivity: Is It Accurate to Use a Slab Ocean Model? *Journal of Climate*, 22(9), 2494–2499. doi:10.1175/2008JCLI2596.1
- Gent, P. R., Danabasoglu, G., Donner, L. J., Holland, M. M., Hunke, E. C., Jayne, S. R., ... Zhang, M. (2011a). The Community Climate System Model Version 4. *Journal of Climate*, 24(19), 4973–4991. doi:10.1175/2011JCLI4083.1
- Gent, P. R., Danabasoglu, G., Donner, L. J., Holland, M. M., Hunke, E. C., Jayne, S. R., ... Zhang, M. (2011b). The Community Climate System Model Version 4. *Journal of Climate*, 24(19), 4973–4991. doi:10.1175/2011JCLI4083.1
- Goldner, a., Huber, M., & Caballero, R. (2013). Does Antarctic glaciation cool the world? *Climate of the Past*, 9(1), 173–189. doi:10.5194/cp-9-173-2013
- Goldner, a., Huber, M., Diffenbaugh, N., & Caballero, R. (2011). Implications of the permanent El Niño teleconnection “blueprint” for past global and North American hydroclimatology. *Climate of the Past*, 7(3), 723–743. doi:10.5194/cp-7-723-2011
- Greenwood, D. (1996). Eocene monsoon forests in central Australia? *Australian Systematic Botany*, 9, 95–112.
- Halley, E. (1686). An Historical Account of the Trade Winds, and Monsoons, Observable in the Seas between and Near the Tropicks, with an Attempt to Assign the Phisical Cause of the Said Winds, By E. Halley. *Philosophical Transactions of the Royal Society of London*, 16(179-191), 153–168. doi:10.1098/rstl.1686.0026
- Harris, N. (2006). The elevation history of the Tibetan Plateau and its implications for the Asian monsoon. *Palaeogeography, Palaeoclimatology, Palaeoecology*, 241(1), 4–15. doi:10.1016/j.palaeo.2006.07.009

- Harrison, T. M., Copeland, P., Kidd, W. S., & Yin, a. (1992). Raising tibet. *Science (New York, N.Y.)*, 255(5052), 1663–70. doi:10.1126/science.255.5052.1663
- Hay, W., Soeding, E., DeConto, R., & Wold, C. (2002). The Late Cenozoic uplift - climate change paradox. *International Journal of Earth Sciences*, 91(5), 746–774. doi:10.1007/s00531-002-0263-1
- Hendon, H. H., & Brant, L. (1990). A composite study of onset of the Australian summer monsoon. *Journal of the Atmospheric ...*, 47(18), 2227–2240.
- Higgins, R., Yao, Y., & Wang, X. (1997). Influence of the North American monsoon system on the US summer precipitation regime. *Journal of Climate*, 10, 2600–2622.
- Holton, J., & Hakim, G. (2012). *An introduction to dynamic meteorology* (4th ed., pp. 86–114). Burlington, MA USA: Elsevier Ltd.
- Hopsch, S. B., Thorncroft, C. D., & Tyle, K. R. (2010). Analysis of African Easterly Wave Structures and Their Role in Influencing Tropical Cyclogenesis. *Monthly Weather Review*, 138(4), 1399–1419. doi:10.1175/2009MWR2760.1
- Huber, M., & Goldner, A. (2012). Eocene monsoons. *Journal of Asian Earth Sciences*, 44, 3–23. doi:10.1016/j.jseaes.2011.09.014
- Hurrell, J., Holland, M. M., Gent, P. R., Ghan, S., Kay, J., J., K. P., ... Marshall, S. (2013). The Community Earth System Model: A Framework for Colloborative Research. *American Meteorological Society*.
- Kapp, P., Murphy, M. a., Yin, A., Harrison, T. M., Ding, L., & Guo, J. (2003). Mesozoic and Cenozoic tectonic evolution of the Shiquanhe area of western Tibet. *Tectonics*, 22(4), n/a–n/a. doi:10.1029/2001TC001332
- Kitoh, A. (2002). Effects of Large-Scale Mountains on Surface Climate. A Coupled Ocean-Atmosphere General Circulation Model Study. *Journal of the Meteorological Society of Japan*, 80(5), 1165–1181. doi:10.2151/jmsj.80.1165
- Kitoh, A. (2004). Effects of mountain uplift on East Asian summer climate investigated by a coupled atmosphere-ocean GCM. *Journal of Climate*, 17, 783–802.
- Kutzbach, J. E., Guetter, P. J., Ruddiman, W. F., & Prell, W. L. (1989). Sensitivity of climate to late Cenozoic uplift in southern Asia and the American west: Numerical experiments. *Journal of Geophysical Research*, 94(D15), 18393. doi:10.1029/JD094iD15p18393



- Lenters, J. D., & Cook, K. H. (1995). Simulation and Diagnosis of the Regional Summertime Precipitation Climatology of South America. *Journal of Climate*, 8, 2988–3005.
- Li, Y., Jourdain, N. C., Taschetto, A. S., Ummenhofer, C. C., Ashok, K., & Sen Gupta, A. (2012). Evaluation of monsoon seasonality and the tropospheric biennial oscillation transitions in the CMIP models. *Geophysical Research Letters*, 39(20), n/a–n/a. doi:10.1029/2012GL053322
- Manabe, S., & Terpstra, T. (1974). The effects of mountains on the general circulation of the atmosphere as identified by numerical experiments. *Journal of the Atmospheric Sciences*, 31(1), 3–42.
- Martin, J. (2006). *Mid-latitude Atmospheric Dynamics A First Course* (2nd ed., pp. 115–145). West Sussex, England: John Wiley & Sons.
- Meehl, G. a., Washington, W. M., Arblaster, J. M., Hu, A., Teng, H., Kay, J. E., ... Strand, W. G. (2013). Climate Change Projections in CESM1(CAM5) Compared to CCSM4. *Journal of Climate*, 26(17), 6287–6308. doi:10.1175/JCLI-D-12-00572.1
- Meehl, G., Arblaster, J., & Fasullo, J. (2011). Model-based evidence of deep-ocean heat uptake during surface-temperature hiatus periods. *Nature Climate ...*, 1, 360–364. doi:10.1038/NCLIMATE1229
- Molnar, P., Boos, W. R., & Battisti, D. S. (2010). Orographic Controls on Climate and Paleoclimate of Asia: Thermal and Mechanical Roles for the Tibetan Plateau. *Annual Review of Earth and Planetary Sciences*, 38(1), 77–102. doi:10.1146/annurev-earth-040809-152456
- Molnar, P., & Emanuel, K. A. (1999). Temperature profiles in radiative-convective equilibrium above surfaces at different heights Peter Molnar surface temperatures decrease -1 , with all other. *Journal of Geophysical Research*, 104(D20), 265–271.
- Molnar, P., & England, P. (1990). Late Cenozoic uplift of mountain ranges and global climate change: chicken or egg? *Nature*, 346, 29–34.
- Neale, R. B., Chen, C., Lauritzen, P. H., Williamson, D. L., Conley, A. J., Smith, A. K., ... Morrison, H. (n.d.). Description of the NCAR Community Atmosphere Model ( CAM 5 . 0 ).

- Nigam, S., Held, I., & Lyons, S. (1988). Linear simulation of the stationary eddies in a GCM. Part II: The “mountain” model. *Journal of the atmospheric ...*, 45(9), 1433–1452.
- Nigam, S., Held, I. M., & Lyons, S. W. (1986). Linear Simulation of the Stationary Eddies in a General Circulation Model. Part I: The No-Mountain Model. *Journal of the Atmospheric Sciences*, 43(23), 2944–2961.
- Oliver, J. (2005). *The encyclopedia of world climatology* (pp. 509–515). Dordrecht, The Netherlands: Springer.
- Plumb, R. A. (2005). Dynamical constraints on monsoon circulations Sustained divergent flows : the circulation constraint in the upper troposphere.
- Prell, W., & Kutzbach, J. (1992). Sensitivity of the Indian monsoon to forcing parameters and implications for its evolution. *Nature*, 360, 647–652.
- Qiu, J. (2013). Monsoon Melee. *AAAs*, 340(June), 1400–1401.
- Ramstein, G., Fluteau, F., Besse, J., & Joussaume, S. (1997). Effect of orogeny, plate motion and land-sea distribution on Eurasian climate change over the past 30 million years. *Nature*, 386, 788–795.
- Rao, G., & Erdogan, S. (1989). The atmospheric heat source over the Bolivian plateau for a mean January. *Boundary-Layer Meteorology*, 46, 13–33.
- Raymo, M. E., & Ruddiman, W. F. (1992). Tectonic forcing of late Cenozoic climate. *Nature*, 359(6391), 117–122. doi:10.1038/359117a0
- Reiter, P. E. R. (1968). Contributions to a Meteorology of the Tibetan Highlands By H. Flohn Department of Atmospheric Science Colorado State University Fort Collins , Colorado Prepared with the support under Grant E-1 0-68G from the.
- Ruddiman, W. (1998). Early uplift in Tibet? *Nature*, 394(August), 6–7.
- Ruddiman, W. F., & Kutzbach, J. E. (1989). Forcing of Late Cenozoic Northern Hemisphere Climate by Plateau Uplift - I EO •, 94.
- Song, X., Zhang, G. J., & Li, J.-L. F. (2012). Evaluation of Microphysics Parameterization for Convective Clouds in the NCAR Community Atmosphere Model CAM5. *Journal of Climate*, 25(24), 8568–8590. doi:10.1175/JCLI-D-11-00563.1

- Stein, T. H. M., Parker, D. J., Delanoë, J., Dixon, N. S., Hogan, R. J., Knippertz, P., ... Marsham, J. H. (2011). The vertical cloud structure of the West African monsoon: A 4 year climatology using CloudSat and CALIPSO. *Journal of Geophysical Research*, 116(D22), D22205. doi:10.1029/2011JD016029
- Sultan, B., & Janicot, S. (2003). The West African monsoon dynamics. Part II: The “preonset” and “onset” of the summer monsoon. *Journal of climate*, 16, 3407–3427.
- Trenberth, K., Stepaniak, D., & Caron, J. (2000). The global monsoon as seen through the divergent atmospheric circulation. *Journal of Climate*, 13, 3969–3993.
- Volkmer, J. E., Kapp, P., Guynn, J. H., & Lai, Q. (2007). Cretaceous-Tertiary structural evolution of the north central Lhasa terrane, Tibet. *Tectonics*, 26(6), n/a–n/a. doi:10.1029/2005TC001832
- Wang, B., & Ding, Q. (2006). Changes in global monsoon precipitation over the past 56 years. *Geophysical Research Letters*, 33(6), L06711. doi:10.1029/2005GL025347
- Wang, B., Wu, Z., Li, J., Liu, J., Chang, C.-P., Ding, Y., & Wu, G. (2008). How to Measure the Strength of the East Asian Summer Monsoon. *Journal of Climate*, 21(17), 4449–4463. doi:10.1175/2008JCLI2183.1
- Wang, P. (2009). Global monsoon in a geological perspective. *Chinese Science Bulletin*, 54(7), 1113–1136. doi:10.1007/s11434-009-0169-4
- Webster, P., & Chou, L. (1980). Seasonal structure of a simple monsoon system. *Journal of the Atmospheric ...*, 37, 354–367.
- Wu, G., Liu, Y., He, B., Bao, Q., Duan, A., & Jin, F.-F. (2012). Thermal controls on the Asian summer monsoon. *Scientific reports*, 2, 404. doi:10.1038/srep00404
- Yanai, M., & Li, C. (1994). Mechanism of heating and the boundary layer over the Tibetan Plateau. *Monthly Weather Review*, 122, 305–323.
- Yanai, M., & Wu, G. (2006). Effects of the Tibetan Plateau. In *The Asian Monsoon* (pp. 70–105).
- Yin, A., & Harrison, T. (2000). Geologic evolution of the Himalayan-Tibetan orogen. *Annual Review of Earth and Planetary ...*, 28, 211–280.

- Zhang, G. J., & McFarlane, N. a. (1995). Sensitivity of climate simulations to the parameterization of cumulus convection in the Canadian climate centre general circulation model. *Atmosphere-Ocean*, 33(3), 407–446. doi:10.1080/07055900.1995.9649539
- Zhang, S., & Wang, B. (2008). Global summer monsoon rainy seasons. *Royal Meteorological Society*, 1578(January), 1563–1578. doi:10.1002/joc
- Zhisheng, A., Kutzbach, J. E., Prell, W. L., & Porter, S. C. (2001). Evolution of Asian monsoons and phased uplift of the Himalaya-Tibetan plateau since Late Miocene times. *Nature*, 411(6833), 62–6. doi:10.1038/35075035
- Zhou, J., & Lau, K. (1998). Does a monsoon climate exist over South America? *Journal of Climate*, 11(1971), 1020–1040.